The $\vec{n} + p \rightarrow d + \gamma$ Experiment at LANL

White Paper for DOE Review, November 5–6, 2002

October 25, 2002

The NPDGamma Collaboration

Contents

1 Physics Overview **1**

2 Background of the Project **2**

3 Summary of Current Status of Work Packages **3**

3.1 Status of the NPDGamma Experiment Construction Project 4

3.1.1 WBS 1.1 — Signal Electronics 4

3.1.2 WBS 1.2 — Data Processing 5

3.1.3 WBS 1.3 — Detector 7

3.1.4 WBS 1.4 — ^{3}He Polarizer 9

3.1.5 WBS 1.5 — Spin Flipper 11

3.1.6 WBS 1.6 — Guide Field 12

3.1.7 WBS 1.7 — LH_2 Target 14

3.1.8 WBS 1.8 — Beam Monitors 17

3.1.9 WBS 1.9 — Cave 18

3.1.10 WBS 1.10 — ER2 Utilities 20

3.2 Status of the NPDGamma Beam Line Construction Project 20

3.2.1 WBS 2.1 — In-Pile Guide 20

3.2.2 WBS 2.2 — Shutter 22

3.2.3 WBS 2.3 — Chopper 22

3.2.4 WBS 2.4 — Integrated Shielding 23

3.2.5 WBS 2.5 — Neutron Guide 24

3.2.6 WBS 2.6 — ER1 Utilities 24

4 Updates to Statistical and Systematic Errors **26**

4.1 Statistical Errors 26

4.2 Systematic Errors 26

4.2.1 Type 1 — Systematic errors of instrumental origin 27

4.2.2 Type 2 — Systematic errors from couplings to the neutron spin 27

4.2.3 Spin Reversal 27

4.2.4 Stability of operating conditions 27

5 Status of Costs and Schedules of the Projects **28**

5.1 Status of Experiment Construction 28

5.1.1 Status of the Budget for the Experiment Construction 28
5.1.2 Major Changes to the Experiment Construction Baseline 30
5.1.3 New Major Milestones to Complete the Project 30
5.2 Status of Beam Line Construction 32
5.2.1 Status of the Budget for Beam Line Construction 32
5.2.2 Major Changes to the Beam Line Construction Baseline 34
5.2.3 New Major Milestones to Complete the Beam Line Construction 34

A NPDGamma Proposal **35**

B Management Plan **35**

C Schedules **35**

D Draft Commissioning and Operations Plan **35**

E Draft Agreement Between Physics and LANSCE Divisions **35**

F Draft Article of Fall 2000 Test Run Results **35**

G Publication List **35**

This paper provides an overview of the status of the NPDGamma ($\vec{n} + p \rightarrow d + \gamma$) construction project at LANSCE, as well as plans for commissioning and operation. It includes:

- a very brief review of the physics of the experiment and background of the project,
- a detailed description of the progress and plans for the construction of the experiment and the beam line,
- an update on estimates of statistical and systematic errors, and
- the status of the budget and schedules.

The final portion of this report is several appendices containing supplementary information.

1 Physics Overview

The NPDGamma experiment will measure the parity-violating gamma-ray asymmetry with respect to the neutron spin when polarized cold neutrons are captured by para-hydrogen. The asymmetry is expected to be very small, approximately -5×10^{-8}. With the LANSCE spallation source it is possible to measure this asymmetry to an accuracy of 1.5×10^{-8} assuming that the experiment is carefully designed and constructed. The experiment will use the pulsed nature of the beam to control systematic errors. A schematic of the experimental setup is shown in Fig. 1. Detailed description of the NPDGamma experiment and the fundamental physics beam line can be found in the proposal "Measurement of the Parity-Violating Gamma Asymmetry A_γ in the Capture of Polarized Cold Neutrons by Para-Hydrogen," (Appendix A).

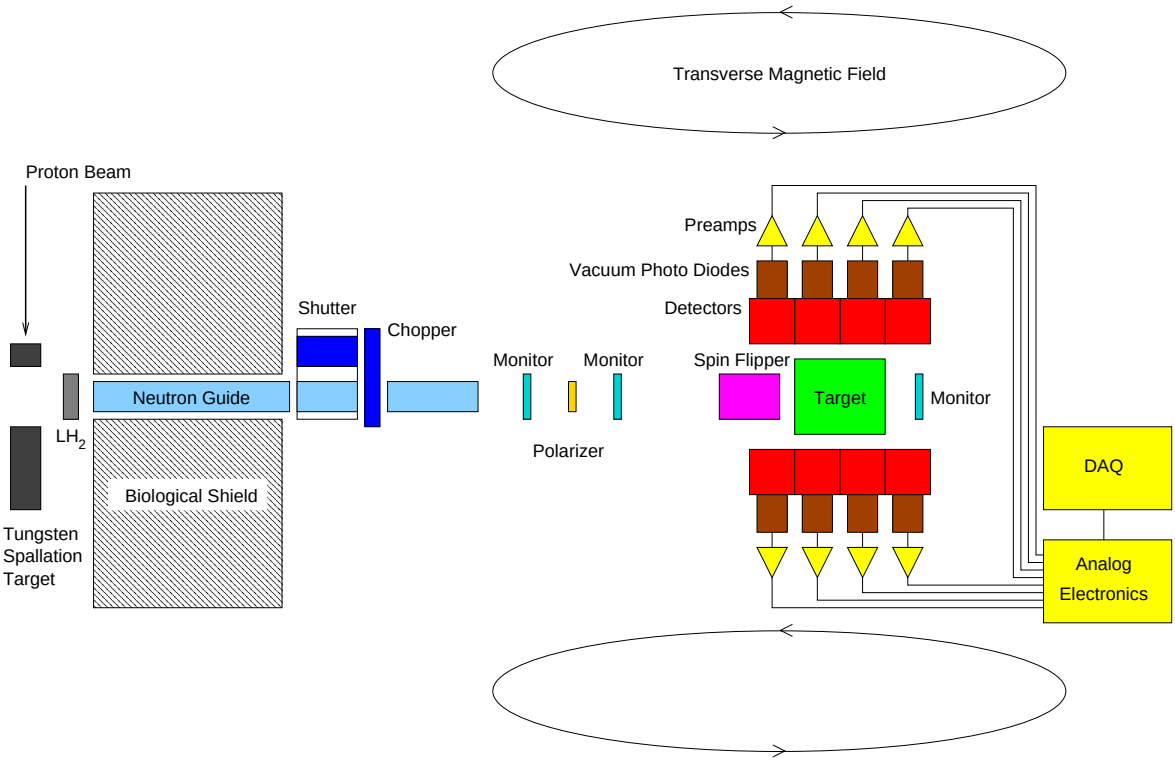

Figure 1: Diagram of the NPDGamma experiment, showing the major components.

2 Background of the Project

The NPDGamma collaboration was formed and the proposal for the experiment written in 1997. The physics of the NPDGamma experiment was reviewed in 1997 by the Pendlebury Committee. In 1998 a technical review of the project was performed by the Spinka I Committee. The result of this review created the cost baseline and schedule baseline for the project.

After the Spinka I Committee validations, the baseline budget and the schedule were presented to DOE. The NPDGamma project (consisting of the construction of the experiment and the beam line) was seeking $2,537k capital funding from DOE. The scheduled completion date included in the validated baseline was November 2001. In 1999 the project received its first DOE capital funds.

Following the Spinka I Committee, the project was divided into two projects: the construction of the NPDGamma experiment and the construction of the beam line. The estimated cost of the beam line was affected by changes at LANSCE. These included the LANSCE spallation neutron source becoming a Category III (CAT III) nuclear facility, the facility tightening its radiological shielding requirements, and the length of the beam line increasing to gain adequate floor space for the experiment. These changes increased the cost estimate and affected the performance of the beam line significantly. This elevated cost estimate triggered a new technical review — the Spinka II Committee that took place in September 2000. The Spinka II review recommended that the NPDGamma project develop a written Project Plan and develop an improved cost estimate based on DOE contingency rates.

After the Spinka II review the NPDGamma collaboration initiated preparation of the Project Management Plan (PMP) as well as the validation of the cost and the schedule for the construction of the experiment and the beam line.

The goal of the PMP was to ensure that the NPDGamma project had:

- formal management in place,
- reliable costs, schedules and contingencies,
- management control in place, and
- appropriate reporting in place,

and that the NPDGamma project meets:

- its design specifications,
- relevant Laboratory ES&H requirements, and
- relevant Laboratory Quality Assurance requirements.

The NPDGamma experiment will be constructed on flight path 12 (FP12) at the Manuel Lujan Jr. Neutron Scattering Center (MLNSC) at LANSCE. In addition to the construction of the experiment, the NPDGamma collaboration must build the beam line for the experiment. The beam line includes the neutron guide, the external shutter, the chopper, and the radiological shielding. Concurrent with FP12 construction, LANSCE division will build FP13. The construction of these beam lines is a collaborative effort between Physics and LANSCE Divisions, coordinated by LANSCE. This integrated construction plan was one of the recommendations of the Spinka I Committee.

3 Summary of Current Status of Work Packages

The beam line and experiment are both progressing well as discussed in detail in the text. We have made a number of measurements to understand the performance of the source, beam line, and apparatus. During the 2001 test run, we found that the photodiodes had magnetic feedthroughs. A careful analysis showed that the potential systematic error from analysis of the circular polarization was negligible. This was our greatest surprise in the area of systematics. All other systematics remain under control. We now expect to measure A_γ with a statistical error of 1.7×10^{-8} in three LANSCE run cycles. At present the highest risk to the success of the experiment is the stray field from the superconducting magnet located on neighboring Flight Path 11A that precludes data taking on Flight Path 12 where the NPDGamma experiment is located. The Physics and LANSCE divisions are working hard to find an administrative solution to the problem in CY03 and CY04 and a long-term engineering solution that will decouple the flight paths in CY05 and thereafter. The draft of the agreement is attached, see Appendix E.

This section provides a summary of current status of construction of the NPDGamma experiment (Section 3.1) and the FP12 beam line (Section 3.2). For reference, the work packages and work package leaders are given in Tables 1 and 2, organized by work breakdown structure (WBS).

WBS	Work package title	Work package leader	Add'l Contributing Institutions
1.1	Signal Electronics	W. S. Wilburn (LANL)	
1.2	DAQ	W. S. Wilburn (LANL)	
1.3	Detector	W. M. Snow (IU)	KEK, LANL, Manitoba/TRIUMF
1.4	Polarizer	K. Coulter (U. Michigan),	NIST, LANL, UNH,
		T. Smith (U. Dayton)	Hamilton College
1.5	Spin Flipper	W. S. Wilburn (LANL)	
1.6	Guide Field	R. Carlini (JLab)	UC-Berkeley
1.7	LH_2 Target	W. M. Snow (IU)	LANL
1.8	Beam Monitors	S. A. Page (U. Manitoba)	
1.9	Cave	W. S. Wilburn (LANL)	
1.0	ER-2 Utilities	W. S. Wilburn (LANL)	

Table 1: NPDGamma Experiment Work Packages.

WBS	Work package title	Work package leader
2.1	In-Pile	J. D. Bowman (LANL)
2.2	Shutter	S. Penttila (LANL)
2.3	Chopper	M. Leuschner (UNH)
2.4	Integrated Shielding	S. Penttila (LANL)
2.5	Neutron Guide	S. Penttila (LANL)
2.6	ER-1 Utilities	W. S. Wilburn (LANL)

Table 2: NPDGamma Beam Line Work Packages.

3.1 Status of the NPDGamma Experiment Construction Project

The NPDGamma experiment construction project includes ten work packages. Eight work packages cover independent components of the experiment; in addition the project includes two work packages for the construction of the experimental cave and utilities for the experiment. The following subsections describe the status of each of the experiment work packages, organized by WBS. Much of the testing for most of the work packages relates to results from test runs on an existing flight path at MLNSC in Fall 2000 and Fall 2001. In Fall 2000, activity centered around a setup with: a ^{3}He polarizer, an RF spin flipper, CsI detectors, and a DAQ. This setup was used to make asymmetry measurements with precision 2×10^{-6}. In Fall 2001, beam monitors were tested and a CsI detector alignment scheme was exercised.

Figure 2 provides a view of the main hardware components of the NPDGamma experiment for reference.

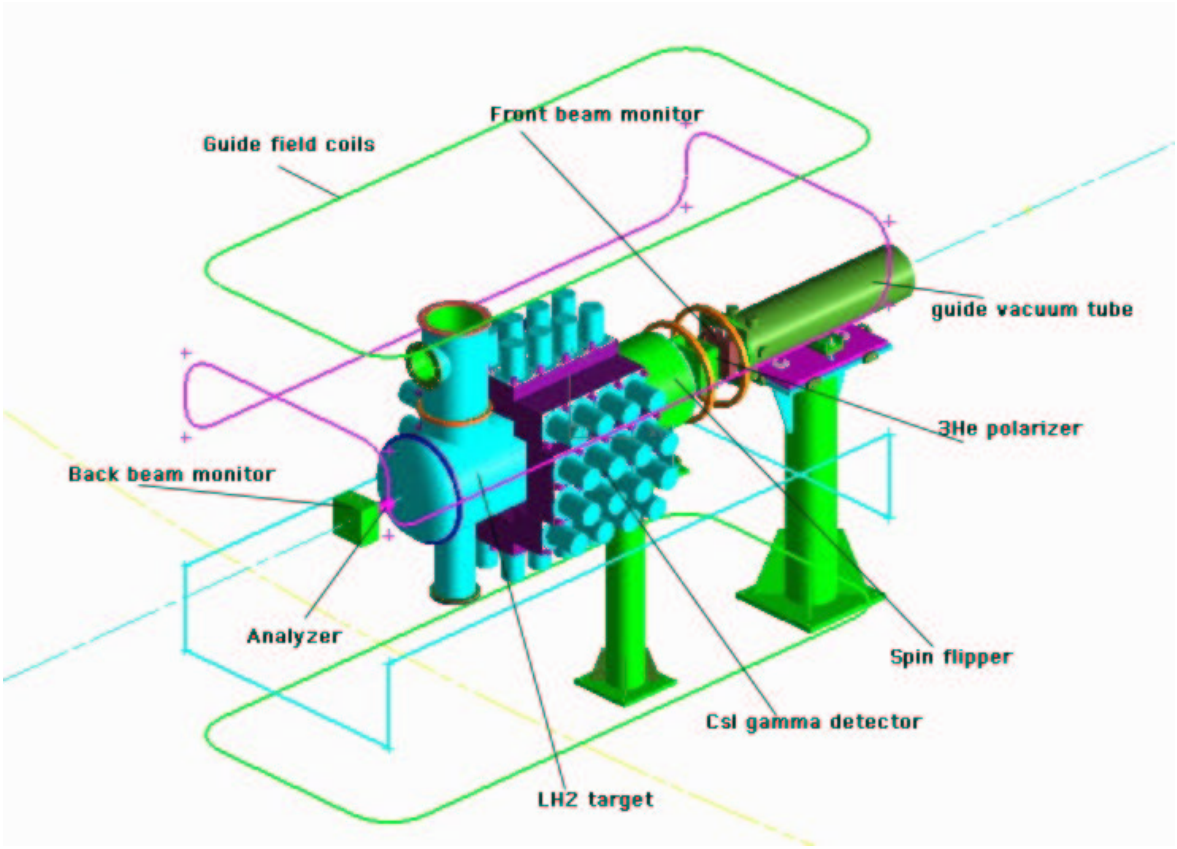

Figure 2: Conceptual picture of the NPDGamma experiment. Neutrons travel along the beam line from upper right to lower left in this figure.

3.1.1 WBS 1.1 — Signal Electronics

The gamma-ray detector consists of CsI(Tl) scintillators viewed by vacuum photodiodes (VPDs) which operate in current mode. The signal electronics convert the anode currents of the VPDs into voltages and process the signals before they are read by the data acquisition system. These functions are divided primarily into two sets of modules: preamplifiers located on the detectors and sum and difference amplifiers (SD amps) located in the DAQ system.

The preamplifiers must convert the photocurrents into voltages without adding significant noise

to the signals. They must have sufficient time response to record the changing gamma intensity over the course of each neutron pulse. Finally, the preamplifiers must be capable of driving output cables connecting them to the SD amps. Solid state preamplifiers were chosen instead of electron multipliers because of their insensitivity to magnetic fields. The 48 CsI detectors are arranged in four rings of twelve. The signals from each ring go to a SD amp which sums the twelve signals and then subtracts this sum from the individual signals, providing twelve difference signals and one sum signal to the DAQ. This process removes common-mode variations from the individual signals, for example from neutron beam intensity changes. This effectively increases the resolution of the ADCs. The SD amps also pass the signals through 6-pole Bessel filters to limit the overall bandwidth and reduce the integrated noise.

A final version of the preamplifier has been tested and meets all performance criteria, achieving a noise of 20 fA/$\sqrt{\text{Hz}}$ (250 times smaller than the shot noise of the signal) and a rise time of 5.7 μs. The noise is dominated by the Johnson noise of the feedback resistor. In addition, the measured results agree with detailed SPICE models of the circuit. All functions of the SD amp have been tested in prototypes and perform as expected.

The preamplifiers are currently being constructed. Housings for the preamplifiers and VPDs are on hand. A final prototype of the SD amp has been ordered. Once the detector stand is constructed and delivered to LANL (expected November 2002), all detectors will be installed with VPDs and preamplifiers in a setup room and tested with the DAQ. The array will be disassembled, moved and reassembled in the cave in April 2003, following the target tests. Operating the signal electronics should require little intervention from the experiment operators. Beam off runs with the detectors illuminated by LEDs will test for multiplicative false asymmetries. Although routine maintenance is not required, repairs can be performed on the preamplifier electronics without removing the detectors from the array.

Because of the extensive prototyping and testing, risks are minimal for the signal electronics. The most critical component, the preamplifier, has been fully tested in its final form. Although a full 12 channel version of the SD amp will not be tested until November 2002, all functions have been individually prototyped and tested.

3.1.2 WBS 1.2 — Data Processing

The data acquisition and processing are implemented in a VME-based system. The system has three crates, each of which has its own CPU. Each VME crate has a companion NIM crate for manipulating logic signals and operating gates for the various VME modules. The VME crate CPUs are coordinated by a desktop PC, and all of the computers use a Linux operating system. The desktop PC gathers the data acquired by each crate and assembles it into run files, which it then writes to tape. The DAQ system needs to reliably record detector data and companion data from the beam monitors and other systems in the experiment.

One of the crates will be located outside the experimental cave, and it will be responsible for gating the T_0's, and for data taken only once per pulse. The other two crates will be located inside the cave, and each will have 48 channels of fast sampling 16-bit ADCs. The detector difference signals will be sent to the second VME crate, and it will have no other inputs to prevent electrical noise pickup. The third crate will read the detector sum signals, as well as the beam monitor outputs and any other signals that require data versus time of flight. The vast majority of data is the fast ADC data, since they will sample at up to 100 kHz. We expect a total data set of 10–20 terabytes for three MLNSC 1L target run cycles.

In the test runs in Fall 2000 and Fall 2001, a DAQ system with one VME crate was used. In Fall 2000 one set of fast sampling ADCs was used to acquire data to measure parity-violating asymmetries in neutron capture on three targets (Cl, Cd, La). The system reliably logged 75 gigabytes over the five-week run, and raw asymmetries were measured to statistical precision of 2×10^{-6}. In Fall 2001 the system was converted from using a Motorola VME controller running pSOS to the VMIC Intel-

based Linux system that will be used for NPDGamma. The system was used to study beam monitor performance and to take data to evaluate a detector alignment scheme.

The status of the DAQ system is as follows. A setup in the lab has three VME crates, three NIM crates, and a desktop PC, as shown in Fig. 3. All VME modules required for the experiment have been purchased and tested. A significant portion of the NIM module logic has been implemented. The VME crates communicate with the desktop PC via fiber optic Ethernet connections, to allow for electrical isolation. Software development has proceeded to the point of controlling the three crates from the desktop PC via Perl scripts and persistent ssh connections. Some minor issues remain with timing and control in the coordination of the four computers. The only remaining item for purchase for the DAQ is a system to archive the data and distribute it to collaborators. Options of DLT data tapes, RAID disk arrays, and CD-ROM/DVDs are being investigated. Data will first be written to local disk and then copied to tape. An archival backup of one of the preceding options will be implemented. The primary focus in development will next move to the analysis software, and this will proceed in parallel with taking bench data with LEDs with the full complement of 48 crystals, VPDs, and preamplifiers when they become available in December 2002. Existing software proved sufficient for the engineering runs but significant work remains to develop software for NPDGamma data analysis.

No obstacles exist to having the data acquisition system ready for detector bench testing at the end of 2002, or to having the system ready to move to ER2 and the experimental cave when they are ready in 2003. Testing the full complement of detectors on the bench will provide an excellent opportunity to develop software and identify possible problems before moving to ER2. Proper functioning of the data acquisition will be required to assess the performance of many components of the apparatus during the installation and commissioning phase of the experiment. Software and documentation will be developed to allow the entire collaboration to have some facility with the system.

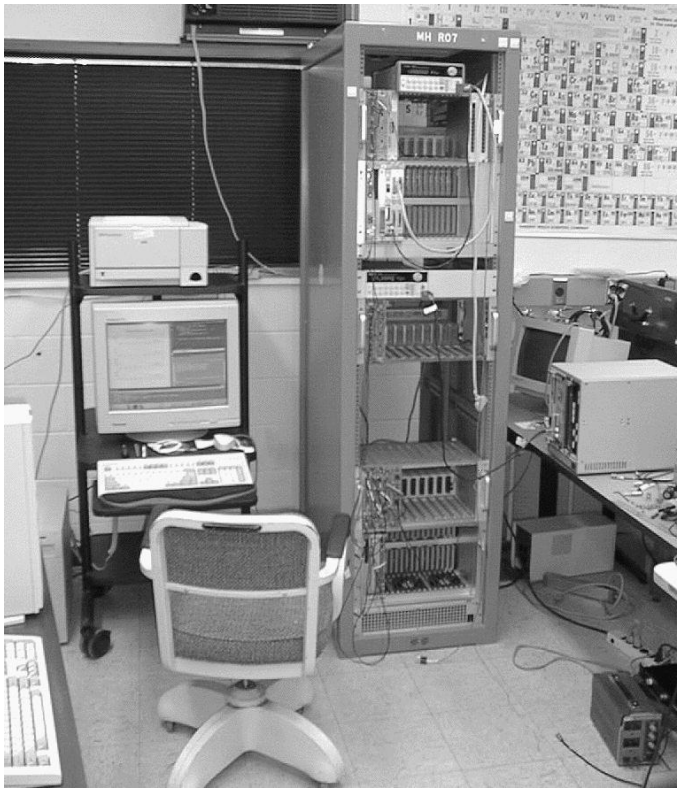

Figure 3: The DAQ setup in the lab at LANL. The tall rack contains two VME crates, and the third VME crate is on the table at the right. The desktop PC is at the left. Each VME crate has a complementary NIM crate for simple logic and gate signals.

3.1.3 WBS 1.3 — Detector

The CsI(Tl) gamma-ray detector consists of 48 CsI(Tl) scintillators viewed by custom designed Hamamatsu VPDs which operate in current mode. The VPDs have low-sheet-resistance S20 photocathodes to insure good linearity. The 2.2 MeV gammas incident on the $15 \times 15 \times 15$ cm^3 CsI(Tl) crystals produce a photocathode current signal in the VPDs. The peak rate of incident gammas per detector will be $\sim 1.5 \times 10^5\,\gamma$/ms, providing peak photocathode currents of $\sim$ 60 nA. The photocathode current signals are converted to voltages by low-noise analog electronics and fed to the DAQ. The array is segmented longitudinally into 4 layers and azimuthally into 12 sectors and is tightly packed around the hydrogen target vacuum vessel. The detectors each possess two LEDs mounted on their corners, for the introduction of test light into the array. Spatial asymmetry in the current mode signal correlated with neutron spin direction is the signature for the parity-violating asymmetry A_γ.

CsI(Tl) crystals were selected for their combination of good stopping power for 2.2 MeV gammas, high light output, acceptably low sensitivity to radiation damage, low magnetic field sensitivity, and cost. The associated VPDs were selected for their good match to the scintillation spectrum from CsI, linearity ($\sim 10^{-4}$), low noise, and insensitivity to AC and DC magnetic fields.

The detector array must absorb at least 90% of the energy from a 2.2 MeV gamma, cover a solid angle of at least 80% of 4π, operate stably to maintain electrical alignment, and possess detectors which produce at least 100 photoelectrons per MeV to ensure a statistical accuracy dominated by capture gamma statistics.

The efficiency of the detector array was simulated (using the EGS4 Monte Carlo software package) and verified in test runs. Average light outputs of 1300 photoelectrons per MeV have been measured with radioactive sources, with variations of $\pm$15%. Measurements of the individual relative efficiencies of the CsI crystals and the VPDs have been completed. The crystals and VPDs will be matched to approach overall uniformity and will be tuned to uniformity in hardware using gain settings in the analog electronics. The uniformity will be monitored throughout the run using the LEDs to illuminate the crystals. Measurements of the sensitivity of the VPDs to DC and RF magnetic fields give the following results: the first derivative of the gain with respect to perpendicular magnetic field is 2×10^{-5}/G, and the second derivative is 1×10^{-5}/G^2. These sensitivities are well below the requirement for the VPDs given expected variations of the fields at the detectors. Measurements in test runs confirm the ability to use the LED signals to quickly check for false electronic asymmetries.

The detectors are electrically isolated from each other and from the mechanical support which fixes them around the liquid hydrogen target. The array stand moves with respect to the hydrogen target to allow overall detector alignment and efficiency tuning. The 48 signals are connected to the DAQ. With flux gate magnetometers, magnetic field mapping and monitoring will be performed on the edges of the array.

The CsI detectors have been procured and delivered to LANL at the end of July 2002, two months ahead of schedule. Michael Gericke, an Indiana University graduate student, has relocated to Los Alamos to work on the array. KEK collaborators have purchased and tested the VPDs, and the VPDs have been shipped to LANL. The testing with a neutron beam at KEK made use of neutron capture on Cd and In targets, to produce gammas to produce light in a CsI(Tl) crystal, onto which each VPD was mounted in turn. The gain variation within the set of VPDs is at the 50% level, as expected. The VPDs will arrive at LANL in November 2002. Assembly of analog electronics will be finished in December 2002. Mounting of the detectors in the array stand has already been tested and will commence in late November 2002. The CsI detector array will be installed in May 2003 after the tests of the liquid hydrogen target. The array will be craned into place through the roof of the cave and mounted onto the stand. Operation with the full assembly in the FP12 cave, using the DAQ, will start in Spring 2003.

The array will be tested with LED signals and radioactive sources using the real DAQ and spin flipper systems before installation into the cave to ensure negligible electrical/mechanical pickup from the spin flipper. After installation into the cave it will be operated using LED light with no beam

to verify negligible electronic noise in the cave. The beam will be used to tune the array efficiency through a combination of detector gain manipulation, array motion, etc.

Both absolute and relative signal intensities from each detector will be monitored throughout the experiment to verify detector stability and the maintenance of the electrical alignment. Beam off with LED light will be used periodically to quickly check for the presence of any false asymmetries from electronic or mechanical pickup. Beam-off periods will be used to verify negligible afterglow and activation of the CsI.

Because the CsI(Tl) crystals have been extensively tested with gammas from neutron capture in previous test measurements, most risks are minimal. The risks will be further minimized by extensive testing in Fall 2002 and Spring 2003 before installation. Motion of the array relative to the hydrogen target will be controlled with mechanical stops in such a way that collision is impossible. The main risk is in the long-term maintenance of the detector array uniformity and electrical alignment. This problem will be addressed by both hardware and software adjustments and periodic monitoring.

A crucial issue for the experiment is the ability to determine the effective detector alignment, *in situ*, to within ± 20 mrad with respect to the vertical magnetic holding field direction, in order to suppress the contribution of a small parity-allowed (left-right) asymmetry to the parity-violating (up-down) asymmetry that we are seeking to measure. An alignment scheme based on scanning a small target within the beam envelope in x and y (x horizontal, y vertical, z is the beam axis) was explored in the Fall 2001 test run. As the source of gamma rays is moved in x and y, the ratio of change in observed signal in a detector versus y motion to the change versus x motion gives the tangent of the angle from vertical of the detector's centroid. This method of scanning the target was found to be unsuitable due to non-uniformities in the beam intensity distribution. As a result, we have concluded that the preferred method to calibrate the detector alignment is to scan the entire detector array in x and y with the liquid hydrogen target in place. This brute-force method places stringent requirements on the detector stand design and construction that were not envisioned when the experiment was originally proposed.

University of Manitoba/TRIUMF collaborators have responsibility for design and construction of an integrated stand for both the CsI detector array and the liquid hydrogen target. The stand will be mounted on a common base plate on top of the cave floor magnetic shielding structure. It will provide for mounting of the CsI array, the RF spin flipper and intermediate beam monitor, the liquid hydrogen target, the rear beam monitor, and the ^{3}He polarization analyzer cell.

A diagram of the integrated stand concept is shown in Fig. 4. An automated motor drive system controlled by the DAQ will scan the detector array in x and y by ± 6 mm when the target is full, to allow for determination of the effective detector alignment offsets *in situ*. The $x-y$ scanner has three independent motion limits to protect the CsI crystals and the hydrogen target: software controls, limit switches, and carriage stop hard limits. The stand also provides for manual retraction of the hydrogen target from the CsI assembly via a set of rails mounted on the base plate.

The construction of the stand relies heavily on crucial engineering and infrastructure support provided by TRIUMF. Conceptual and engineering design studies were carried out during Summer 2002, as well as a most of the machine drawings for fabrication. Before the stand can be completed, the design of the cave floor must be finalized, as this impacts the stand height. Assuming that a solution to the cave design for magnetic shielding is found in time, the stand project will remain on track for delivery to LANL in December 2002. University of Manitoba shops have recently completed fabricating components of the upper CsI array support structure. A completed support panel was shipped to LANL in September 2002, where it was mounted with detectors and preamplifiers; deflections under load were measured to be within tolerances, as predicted by a finite element analysis at TRIUMF. A Co-op student, Justin Ho, has been hired at TRIUMF to work on assembly of the stand elements and programming and testing of the remote $x-y$ controller during Fall 2002.

Our approach to minimize risks associated with the stand project has been to perform a thorough engineering design study, followed up with careful measurements and test fitting of components,

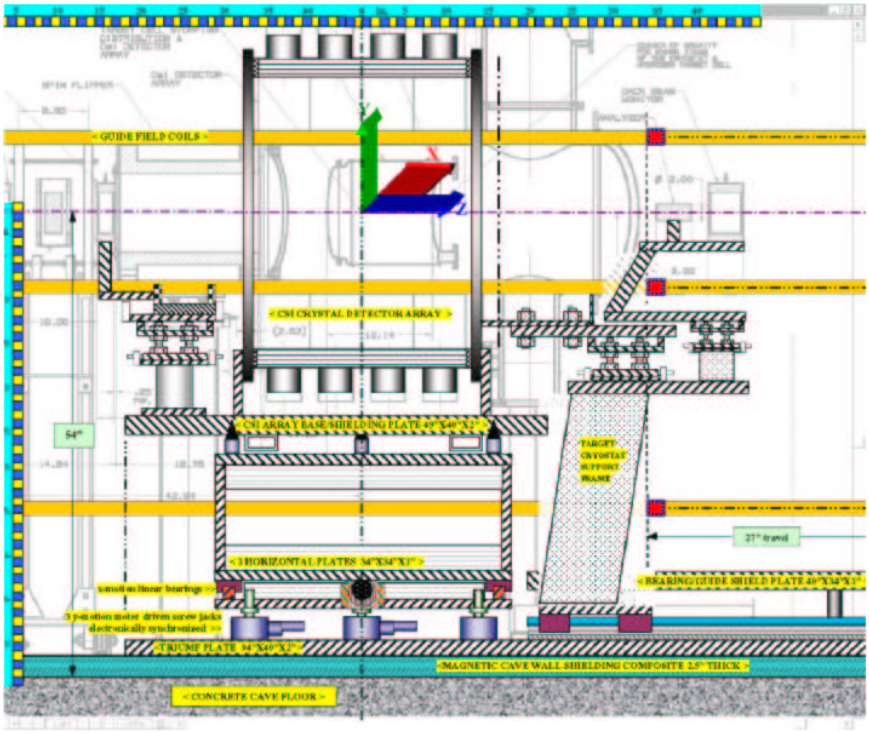

Figure 4: Layout of the integrated detector stand assembly.

and intermediate assembly and testing at TRIUMF including accurate survey measurements as the controller is tested. Once the stand has been shipped to LANL, we will finally recheck all remaining tolerances and test fit the target vessel. Additional survey measurements will be made while the $x-y$ controller is exercised in a setup area at LANSCE prior to installation in the FP12 experimental cave.

3.1.4 WBS 1.4 — ^{3}He Polarizer

This work package has two components: a neutron polarizer and a neutron analyzer.

Polarizer

The neutron polarizer is a polarized ^{3}He spin filter, which presents multiple advantages over its most likely alternative, a polarizing supermirror. The spin filter is a broadband large-phase-space device, providing significant polarization both below and above 15 meV, thus allowing important systematic tests to be carried out. A supermirror is typically only effective for polarizing neutrons of energy less than 9 meV. The ^{3}He spin filter produces negligible gamma ray background, in contrast to a supermirror. The ^{3}He polarization can be flipped independently from the magnetic field, providing an additional flip of the neutron spin for studies of systematic effects. Finally, because the spin dependent ^{3}He absorption cross section has a $1/v$ dependence, the beam polarization can be determined from the measured transmission through the spin filter.

The polarizer system has five components: the cell, the cell oven and its air heater system, lasers and optics, NMR polarimetry, and a stand. These components have been designed and built at different member institutions as described in the following paragraphs. The entire set-up is being assembled at the University of Michigan, and will be sent to Los Alamos in early 2003.

The spin filter cells are constructed of boron-free GE180 glass and have diameter 11 cm, which is sufficient to capture $> 80\%$ of the 9.5×9.5 cm^2 FP12 beam. The ^{3}He thickness, about 5 cm at 0.9

bar, is optimized for expected ^{3}He polarization and the energy spectrum of the FP12 beam. Optical pumping spin exchange is used to polarize the ^{3}He. Several ^{3}He cells have been constructed at NIST, and the present inventory includes one 11 cm diameter and three 10 cm diameter cells with very long polarization lifetimes. (Long polarization lifetime is essential for high ^{3}He polarization, because it balances the spin-exchange polarization times of many hours.) In two of the cells the wall relaxation times approach the theoretical limit given by ^{3}He dipole-dipole spin relaxation. Polarization of $57\pm3\%$ has been measured in the NIST test set up with 60 W of broadband laser diode power.

The oven and its heater system have been constructed at the University of Dayton. The oven is a more complicated system than typically used for Rb-^{3}He spin exchange systems because of the noise restrictions on electronics placed in the cave. The oven and heater are undergoing testing at the University of Dayton and will be sent to the University of Michigan for integration and polarization testing in November.

The lasers and optics components are undergoing testing with a 11 cm ^{3}He cell at the University of Michigan. Two independent 30 W laser diode systems (from Coherent, Inc.) are used to polarize the cells. One laser will pump from above and one from below the cell. All lasers and optical equipment have been procured.

An NMR system will be used for diagnostics on the ^{3}He spin filter, and to flip the ^{3}He spin during the run. The NMR polarimetry system has been constructed at Hamilton College. It is a standard adiabatic fast passage (AFP) NMR system with a few enhancements: it functions through optical fiber links for GPIB and FireWire, also due to in-cave noise restrictions, and it has the capability of running either a field sweep or frequency sweep. Frequency sweep will be used during the experiment, allowing the main guide field to be kept constant. The polarimetry system will be delivered to the University of Michigan in October 2002.

The stand design uses stock aluminum rail components. The stand will be constructed during November 2002 at Michigan. The stand will place cell, oven, and optics in the allotted space of 30 cm on FP12.

Tests in November 2002, at the University of Michigan with the full spin filter apparatus (except the large guide coils), aim to achieve high polarization and validate all system components. The figure-of-merit for the experiment is linear with ^{3}He polarization, and we require at least 50% ^{3}He polarization to attain the proposed statistical error. Polarizations greater than 50% have been demonstrated with spin filter cells at NIST, and this performance is anticipated at Michigan. Equal or better performance is expected at Los Alamos, because other polarization limiting factors (*e.g.* magnetic field gradients) will be less in the cave.

Following the November 2002 tests of the complete system, the polarizer will be transported to Los Alamos and assembled in the laser lab in January 2003. Long term reliability will be further tested at LANL. Compatibility of the NMR with the neutron beam monitors and the RF spin flipper will also be tested. The system will then be moved onto the FP12 beam line in Spring 2003. Because the ^{3}He polarizer will sit on its own stand and the ^{3}He oven can be slid out of the beam, mechanical integration questions have been minimized. During set-up, we will use *in-situ* NMR polarimetry of ^{3}He . During the run, neutron polarimetry will use the transmission difference through the ^{3}He measured by the thin neutron beam monitors (described in Section 3.1.8). The energy dependent ratio of the monitor fluxes will provide a measure of the product of the ^{3}He polarization and the filter opacity, and by inference the neutron polarization. The working spin filter is required for the commissioning of the RF spin flipper and the ^{3}He analyzer.

Analyzer

We require a separate neutron spin analyzer down stream of the target/detector assembly to characterize and monitor the RF spin flipper and to confirm the expected energy dependence of neutron polarization after the para-hydrogen target. In earlier test runs, a supermirror was used as a neutron spin analyzer. However, the magnetic field from a supermirror is not compatible with several

experimental requirements. A small polarized ^{3}He cell will be used as the neutron spin analyzer for the experiment. The cell will be used to sample small portions of the neutron beam, thus measuring and verifying spin flipper performance across the beam profile.

The ^{3}He neutron analyzer is being designed at the University of New Hampshire. It will make use of several components at Los Alamos, including existing high pressure ^{3}He cells. In November these components will be transferred to New Hampshire for the construction and testing of the analyzer. During the commissioning and operation of the experiment, the analyzer cell will be kept polarized in the laser lab and when needed the cell will be transported to the experiment. Because of the potential for the analyzer to produce false asymmetries, it will be removed during asymmetry runs.

3.1.5 WBS 1.5 — Spin Flipper

Neutron spin reversal provides one method for the control of systematic errors. Spin reversal can be accomplished by changing the polarization direction of the ^{3}He spin filter, by changing the polarity of the 10 G holding field, or on a 20 Hz pulse-by-pulse basis using a resonant spin flipper. Raw experimental asymmetries are calculated in the detector response between states of opposite neutron spin incident on the hydrogen target, for example between spin flipper on and spin flipper off states. Different systematic errors have different responses to the three reversal methods.

The spin flipper consists of an RF solenoid, with its axis oriented along the beam direction. The spin flipper solenoid is mounted in an aluminum can to contain its AC magnetic field. When energized, the spin flipper applies an AC magnetic field, $\vec{B}_1(t)\cos(\omega t)$, perpendicular to the DC vertical 10 G magnetic guide field. The frequency of the AC field, $\sim$30 kHz, is determined by the neutron gyromagnetic ratio and the magnitude of the guide field. The combination of the two fields rotates the neutron spins. The amplitude $B_1(t)$ of the AC field must fall as $1/t$ during each neutron pulse to rotate by π the spins of neutrons of each energy. This $1/t$ dependence is given by the time it takes the neutrons of each part of the time of flight spectrum to travel the length of the spin flipper. The spin flipper is efficient over a wide range of neutron energies.

The RF spin flipper was selected because the experiment is very sensitive to DC magnetic field gradients. Because the neutron beam is pulsed, with neutron time of flight and arrival times corresponding to neutron energy, we can use a spin flipper with no DC field gradient and a time-varying AC amplitude.

The efficiency for spin reversal, averaged over the spatial extent of the neutron beam and the range of energies of interest, must be greater than 90%, both to preserve statistical precision and to keep the observed asymmetry well above expected systematic effects. This efficiency must remain constant over time, with any deviations less than 2%, to keep the systematic error due to uncertainty in the neutron polarization well below the statistical uncertainty. The amplitude of the spin flipper AC magnetic field at the VPDs must be less than 5 mG to not induce a false asymmetry in the detector signals. We will verify this condition both in bench tests and *in situ*.

In the Fall 2000 test run, we measured the efficiency of a preliminary version of the spin flipper as a function of neutron energy and spatial position. The results are in good agreement with our calculations, giving an efficiency of 98% averaged over the beam. Efficiency is defined as the ratio of neutron beam polarization with the spin flipper on versus polarization with it off.

The current and voltage applied to the solenoid are monitored by the data acquisition system. The spin sequencer is triggered by the gated T_0 signal produced by the DAQ. The spin sequence is also monitored by the DAQ. Power for the flipper is obtained from the electrical utilities within the cave. Mechanically, the spin flipper fits partially inside the detector and is supported by the detector stand through an electrically insulating support.

The final version of the spin flipper is currently being constructed. All electronic components exist and the solenoid has been rewound. The electrical and magnetic parameters of the coil are being

verified. Measurements of magnetic field leakage will be used to optimize the thickness of the entrance and exit windows. Stability and operation in proximity to the detector area will be verified before installation and commissioning.

The spin flipper will be installed in May 2003, once the detector stand is in place in the cave. The flipper can easily be lifted and positioned by two people, though it is desirable to support it by a sling attached to the cave ceiling to minimize the risk of damage to adjacent equipment.

The spin flipper will be tested with no beam, to verify pickup in the VPDs and other apparatus is negligible. It will then be operated with polarized beam and the analyzer in place to tune the operating parameters and verify the spin reversal efficiency. The efficiency as a function of position will be measured by scanning the analyzer across the beam profile.

The current profile needed for operating the spin flipper will be generated each beam pulse, and either sent to the solenoid or a dummy load by the spin sequencer. Current and voltage to the solenoid will be continuously monitored to verify stable operation. The DC magnetic field will also be continuously monitored since it directly affects the efficiency. Periodically, the ^{3}He analyzer will be used to directly verify the spin-flip efficiency. In addition, a CCl_4 target will be used to observe the large and known parity-violating asymmetry in neutron capture by chlorine. Beam-off periods will be used to verify that false asymmetries are not produced by the operation of the spin flipper.

Because the spin flipper was extensively tested during the Fall 2000 test run, most risks are minimal. In addition, since the operation of the device is well understood, the planned electrical and magnetic tests before installation will further mitigate these risks. The most significant remaining risk is from changing magnetic fields which will directly affect the spin reversal efficiency. This risk can only be addressed by a combination of magnetic shielding and control of sources of magnetic fields. Stable performance of the spin flipper requires the DC magnetic field at the device change by less than 6 mG.

3.1.6 WBS 1.6 — Guide Field

The guide field system consists of large (3×1.5 m^2) coil assemblies which establish a uniform 10 G field over all experimental components, as shown in Fig. 2. A design with four large coils was chosen to give maximum access to the experimental components, while still producing sufficiently uniform fields. The coils were designed with the iron shielding of the cave taken into account and with the winding ratios adjustable by changing taps to allow for limited cave dimension design changes. The main coils were designed to provide by themselves a high quality homogeneous field appropriate for the final experiment. The two outer coils are approximately one meter above and below the beam line and carry about 60% more current than the inner coils which are about 20 cm above and below the beam line. The system has six additional low current shim coils to handle contingencies and compensate for small residual gradients that might be induced. Fig. 6 shows the range provided by the large number of combinations of windings available on the primary coils, without needing to employ any shimming coils. The coils are wound on rigid frames of 5×5 cm^2 aluminum channel with 6 mm walls.

High quality 25 A, 50 V Danfysik power supplies were chosen to give stable 10 ppm operation and easy field reversal. All power supplies are digitally programmable via front panels and by RS232 connections for absolute reproducibility. A fiber based multiplexer was chosen for sending the RS232 signals into the cave so that no external noise would be introduced. A schematic of the system is shown in Fig. 5.

Bartington flux gate magnetometers were selected as field monitoring devices because of their capability to deliver better than 0.1 mG resolution. The field value will be read back by two 3-axis magnetometers with a precision of 0.1 mG, placed above and below the RF spin flipper for constant field monitoring. The specifications for field gradients are: dB_z/dz less than 1 mg/cm over the LH_2 target and RF spin flipper regions and $dB(\text{transverse})/dr$ over the ^{3}He region held at less than 1 mg/cm. Optimizations of the field based on computer modeling gave gradient values three times

better than the above requirements.

The coil forms, windings and electrical connections from the coils to their junction boxes have been completed. The main power supply and two magnetometers have be acquired and tested. The shim supplies, digital magnetometer readout and fiber optic link have been ordered. The RS232 interface card has been acquired. The guide field stand has been designed and material is being procured.

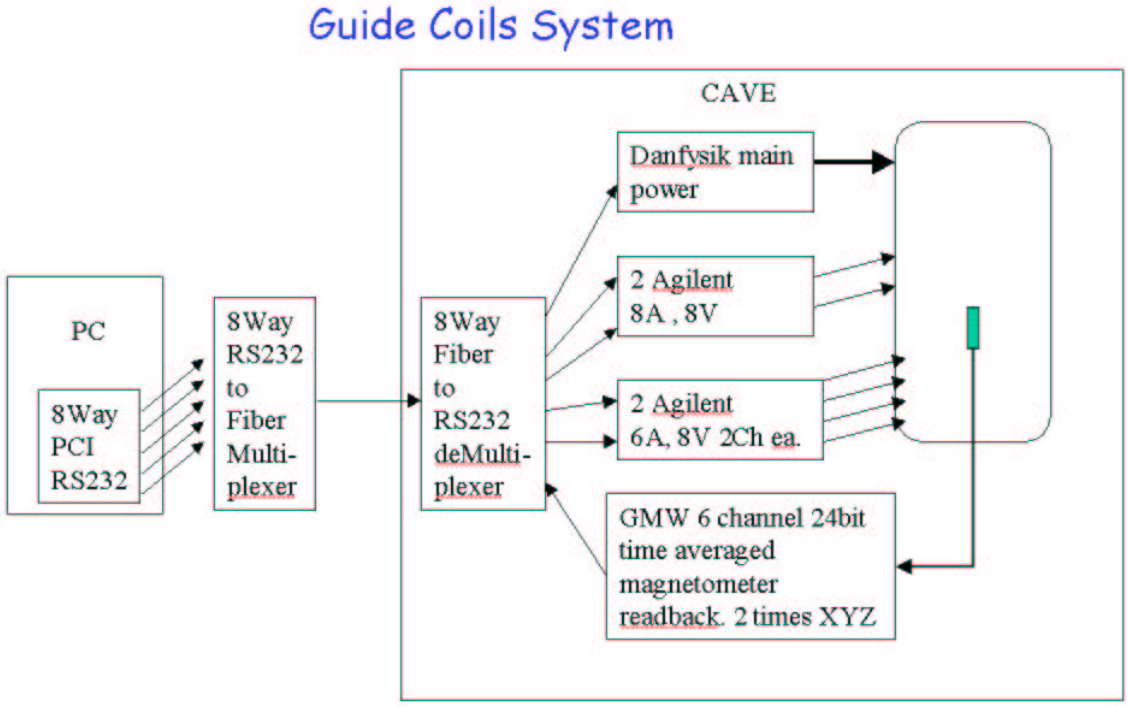

Figure 5: Guide field control system.

The guide coils are on schedule to be installed in the empty experimental cave in April 2003. The magnetometers will be placed at reproducible positions (based on precision holes on the coil forms) to measure initial homogeneity. Initial shimming calculations will be done and applied. Field scans will be repeated until design homogeneity is met. The guide coils may, if required, be partially disassembled to allow other components to be installed more easily. After the complete experimental apparatus has been installed the field will be measured at accessible points to confirm the required homogeneity has been obtained. Sensitive detector systems can be operated with the guide field on and off to search for any interference. Normal EMF shielding techniques will be applied to the power supplies and read back if there are problems. In operation the field above and below the RF spin flipper will be monitored for variations. The guide field control system can change the field polarity.

An obvious risk factor is that the as-built cave dimensions might differ from the dimensions used in the coil optimization. We have minimized this risk by constructing the coils with a set of taps to change their effective winding ratios. In this way, if a re-optimization of the coil spacing or current ratio is called for, the system can be readily reconfigured. The overall risk that acceptable fields cannot be achieved by the present guide coil system appears small. A risk factor is that residual fringe fields might produce a too complex set of gradients to shim out. The magnetic shielding calculations for the cave have indicated that the gradients should be below this requirement.

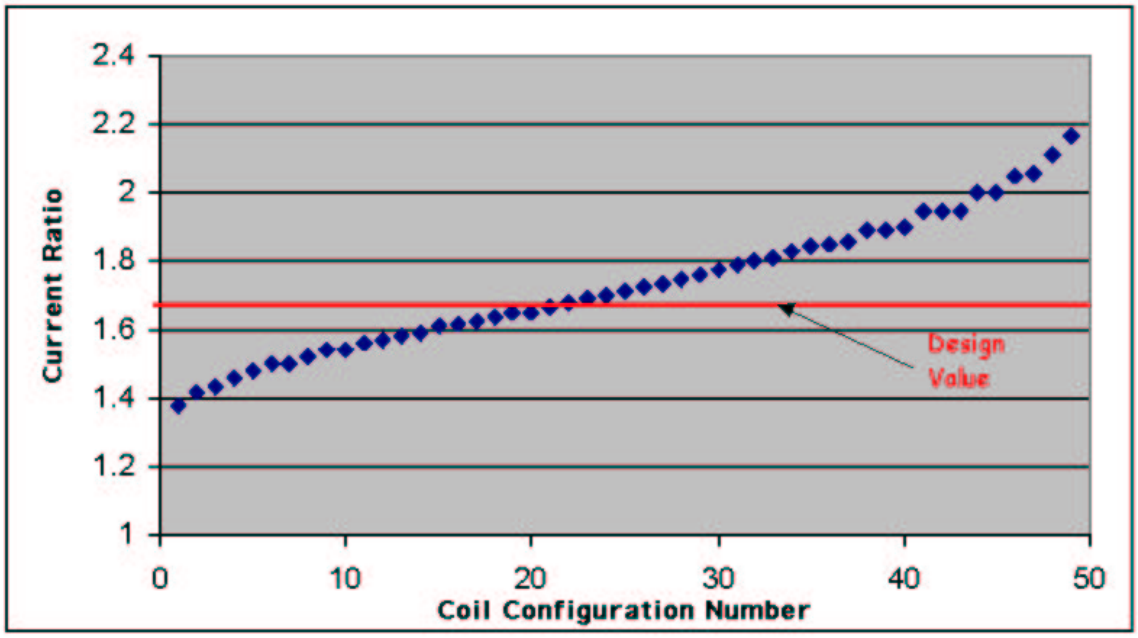

Figure 6: Current optimization with different coil configurations. The x-axis represents a particular combination of windings on each of the four main coils. The indicated range is achievable without invoking shim coils. The plan is to minimize the current in any shim coils by selecting the best initial settings on the main coils.

3.1.7 WBS 1.7 — LH_2 Target

The liquid hydrogen target for the experiment has been designed to meet the physics requirements and to be safe and reliable to operate. The target consists of a 20 ℓ cylindrical titanium chamber filled with liquid para-hydrogen at 17 K. It is liquefied, converted, and cooled with two mechanical refrigerators and an ortho-para converter also held at 17 K. The target chamber is shielded on the outside with lithium-loaded plastic to prevent scattered neutrons from activating the CsI detectors. The vacuum chamber for the target is a welded aluminum assembly with concave magnesium windows for the neutron beam. It possesses helium gas volumes which are exposed to all seals and weld joints so that the main vacuum can be monitored for helium leaks. It is supported on a stand behind the CsI array which possesses rails that can be used to move the target out of the array. The plumbing and vent stack emerge vertically from the vacuum chamber and pass through a hole in the cave roof, where the vent system and gas handling system are located. The pressure and temperatures of the system are monitored by a PLC control system which controls the target operation and will send status information to the facility. A cross-section drawing of the target is shown in Fig. 7.

A pure hydrogen target is required to ensure that any observed asymmetry is due to $n-p$ capture only. A liquid target possesses enough density to localize the source of capture gammas and the para-hydrogen state can be maintained through recirculation through the converter. Only mechanical refrigerators are acceptable given the long-term operation required for the target.

The target must capture 65% of the incident neutron flux. It must be constructed of nonmagnetic materials and not lead to systematic effects due to polarized neutron capture on other materials. It must possess a concentration of ortho-hydrogen of less than 0.05% to ensure less than 1% neutron depolarization due to scattering before capture. It must not possess any thermodynamic fluctuations that lead to noise in the gamma signal greater than counting statistics: this means no bubbles and 0.1 K temperature stability. Finally, it must meet the safety requirements of the facility, among which is the requirement that no hydrogen is released into the cave upon either a loss of vacuum or a internal

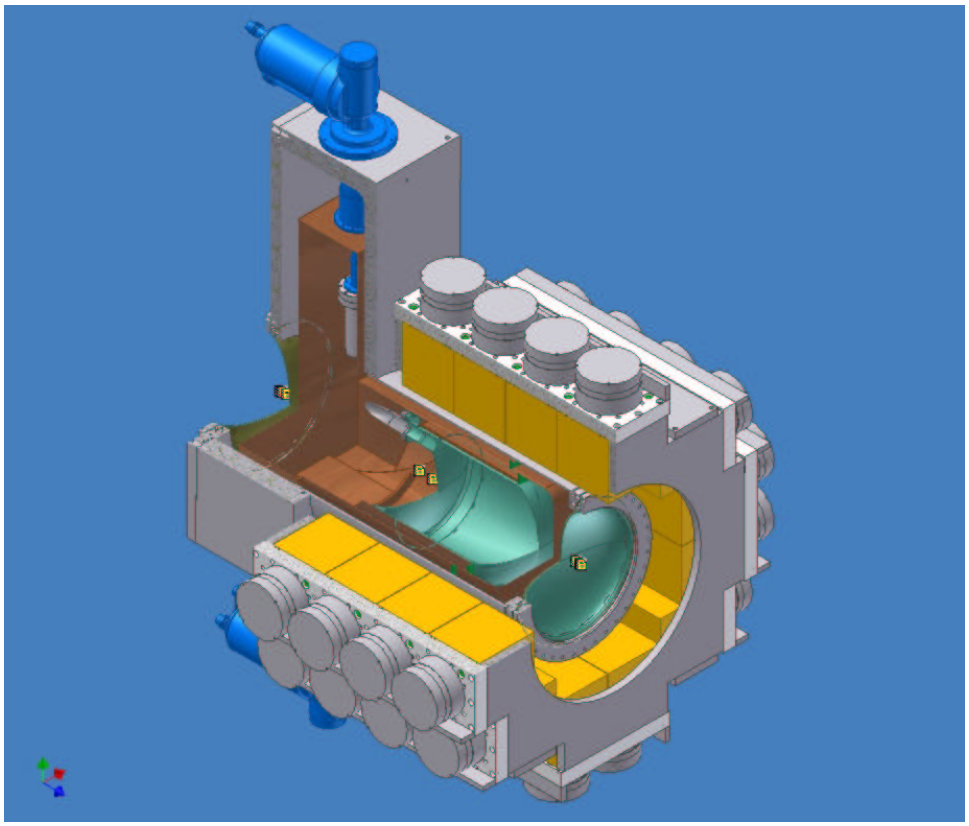

Figure 7: Cutaway drawing of the LH_2 target. Neutron beam direction is lower right to upper left. The 20 ℓ chamber in in the center of the figure. A cutaway of the CsI detector array is shown surrounding the target.

rupture of the target vessel.

The hydrogen target is under construction and there is no operational experience yet. The target is designed to meet all the above criteria. The fraction of neutrons captured has been calculated with Monte Carlo using the predicted neutron spectrum and the known double differential cross section of neutrons from ortho-para mixtures. Magnetic fields from the refrigerator motors have been measured and do not cause a significant magnetic field gradient at the neutron beam. Materials for the target have been chosen based on an analysis of systematic effects from polarized neutron capture on materials with subsequent bremsstrahlung from parity-violating beta decay. For example, the entrance windows of the cryostat and the hydrogen vessel have been made from titanium, which has a very small neutron capture cross section. Because titanium is strong and welds well, its use has increased the overall reliability and safety of the target. The ortho-para ratio at 17 K in thermal equilibrium is below the required 0.05%. This ratio will be measured using the neutron beam monitors and the known neutron cross sections of ortho and para-hydrogen as a function of neutron energy. Bubble formation in the target is suppressed by operating the target at a pressure (1 bar) that is greater than the equilibrium vapor pressure (1/4 bar at 17 K). Standard ASME criteria have been used to design the target vessel and the inlet and outlet lines to ensure acceptable internal pressures during accident scenarios. The design of the target has been approved by a LANSCE hydrogen safety committee.

The target is positioned inside the CsI array and rests on a stand behind the array. It is connected to a relief and gas handling system and to hydrogen bottles outside ER2. It is controlled by a PLC system which reports required information to the facility and the DAQ.

The target is under construction. The main vacuum system and the target chamber are being machined. The final design of the gas handling and relief system will be sent to the safety committee for approval. The rest of the target and controls will be constructed at IUCF. The entire device will be assembled, leak checked, pressure tested, filled with liquid nitrogen/neon for accident scenario simulations, and controlled by the PLC system before transfer to LANL.

The hydrogen target will be installed in the cave in April–May 2003 shortly after the magnetic field coils are installed and tested. It will then be operated with liquid hydrogen for the first time. After initial installation the vacuum chamber will be left in place and parts of the target will be removed as needed for subsequent tests of other systems. Safety reviews of the target operation will be complete before target testing.

The target will be operated without neutron beam to establish the effectiveness of the target filling, control, and vent systems. When neutron beam is available, the effectiveness of the neutron shielding and of the ortho-para converter will be verified. The noise of the gamma signal will be analyzed to verify that there is no extra noise due to target bubbles. Some collaborators will be trained to be target operators who fully understand target operation.

The target will be controlled and monitored by the PLC system. Events which cause the target conditions to exceed preset limits of either safety or experimental parameters will produce alarms that will summon the person on-call. The target will be vented and refilled during long beam shutdowns. Periodic leak checks and gas handling system maintenance will be performed.

The two main classifications of risks are in the safety of the target under various accident scenarios and the risk to the experiment of reliable target operation. Target safety has been the most important component of the design from the beginning and the target cannot be operated until a thorough analysis and verification of safety of design and operation is complete and approved. The target design has been reviewed by two hydrogen target safety review committees charged by LANSCE. The first review was the safety of the conceptual design of the target. The second review dealt with the actual design of the target cryostat. The coming safety reviews will look at the operational safety of the target and the readiness of the target. The target has also been designed for long-term, reliable operation. Reliability of critical items such as the PLC system and the cryo-refrigerators is based on past IUCF experience.

3.1.8 WBS 1.8 — Beam Monitors

Three beam monitors are required for the experiment, as shown in the schematic Fig. 1. These devices are required to provide continuous on-line monitoring of the incident cold neutron flux, of the status of the ^{3}He spin filter, and of the liquid para-hydrogen target during data taking, as discussed below. To meet the needs of the experiment, the beam monitors must provide a low-noise current signal proportional to the neutron beam intensity, with a fast time response for accurate measurement of the neutron time of flight spectrum. They must be insensitive to gamma rays and should produce minimal background in the main detectors. The upstream monitors should introduce the minimum material into the beam path that is consistent with obtaining an acceptable signal. The monitors must be simple, robust, and insensitive to mechanical vibrations; they must not contain magnetic materials that could perturb the magnetic guide field along the flight path through the apparatus or generate a false asymmetry due to interactions with polarized photons.

The design selected for the experiment is based on a simple parallel-plate ionization chamber filled with a gas mix consisting of ^{3}He, ^{4}He, and N_2. A current signal is derived from the sum of the ionization collected when neutrons are captured on the ^{3}He in either of two central 1 cm ionization gaps surrounded by high voltage foils. The total thickness of aluminum, comprising the outer box and inner electrode foils, is 3.5 mm; the beam enters normal to the electrode assembly. The active area is 12×12 cm^2. The reason for choosing a relatively heavy filler gas is to maximize the energy that is deposited in the sensitive region. The intrinsic response time for these detectors will be of order 80 μs when operated at -5 kV; the time response of the signals will be limited by the $I-V$ preamplifiers, which are identical to those used for the main CsI detectors apart from the overall gain. During data taking, the beam monitors will be read out by the fast sampling ADCs in the DAQ.

The ^{3}He capture reaction is ideal for our purposes because it gives 0.77 MeV to the reaction products (p,t) and produces no gamma rays. The front monitors will absorb 1% of the beam at 4 meV to produce a signal, while the back monitor will absorb 50% at 4 meV. This corresponds to a ^{3}He partial pressure of 22 Torr in the front monitors and 380 Torr in the back monitor. All three monitors will be filled to one standard atmosphere and will contain the same partial pressure of N_2, with the remainder made up by ^{4}He in the front monitors. With this choice of gas filling, all monitors can be run from a single high voltage supply and are guaranteed to have the same time response, which simplifies a comparison of the measured intensity profiles.

Not all of the kinetic energy released contributes to the ionization signal, because of the finite detector geometry. The additional noise due to the variance of the energy deposited per neutron E is given by $\sqrt{1+(\sigma_E/E)^2}$. The average energy deposited per captured neutron and its variance were predicted in a numerical simulation as part of a design study. The monitors should have a mean energy deposited of 0.41 MeV with a variance of 0.20 MeV, corresponding to an acceptable intrinsic noise enhancement of 1.1 compared to counting statistics.

During 2001, a prototype beam monitor was built to our specifications by LND, Inc. of Oceanside, NY, and filled with a 50–50 mix of ^{3}He and N_2 at 1 standard atmosphere. The monitor was tested in the cold neutron beam on FP11A at LANSCE. We measured the sensitivity and intrinsic noise of this device in comparison to an existing ^{3}He/^{4}He gas filled ionization monitor and compared the absolute sensitivity to measurements with a collimated beam using a ^{6}Li-doped scintillation detector. The absolute sensitivity and intrinsic noise were confirmed within 10% of the predicted values, considered excellent agreement for the test run setup. The monitor signals were stable, robust, and remarkably insensitive to vibrational pickup. A sample digital oscilloscope trace from the Fall 2001 test run is shown in Fig. 8.

Based on the successful test run data, we placed an order with LND, Inc. for three additional beam monitors that will be used for the experiment. They were filled according to our specifications with appropriate He/N_2 gas mixtures. These monitors were delivered to LANL in October 2002 and will be tested with a neutron beam in November–December 2002. The original prototype monitor, which can be refilled to any desired gas mixture, will be kept as a spare. During commissioning, we will mount the three beam monitors on temporary stands and recheck relative gain and noise characteristics.

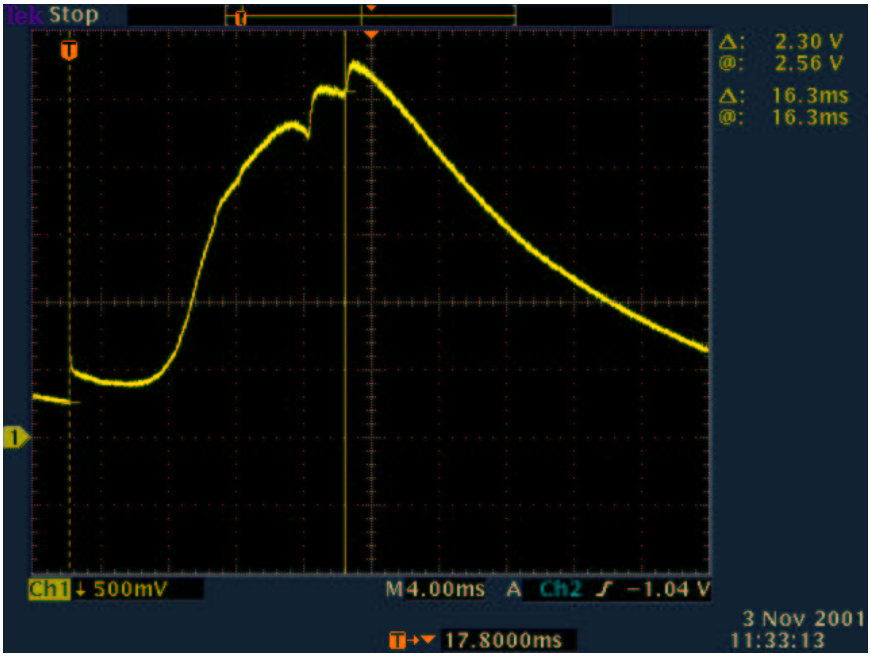

Figure 8: Digital scope plot from the prototype beam monitor during the Fall 2001 test run on LANSCE FP11A. The trace is averaged over 10 beam pulses at 55 μA incident proton current. The current-to-voltage preamplifier had a gain of 5.0 MΩ. No frame overlap chopper was used.

When the full apparatus is installed in the cave, the upstream monitor will be mounted on an insulating bracket at the end of the neutron guide, while the intermediate monitor will be similarly mounted on the upstream face of the RF spin flipper, and the back monitor will be mounted on the integrated LH_2 detector support stand. Transmission measurements of the ^{3}He polarizer cell will be carried out with the cell polarized, unpolarized, and an empty cell, for calibration purposes. Since the cell transmission is a function of both the ^{3}He polarization and thickness, with a known dependence on the beam energy, *in situ* transmission measurements derived from the upstream beam monitors can be combined with ^{3}He NMR polarization measurements to monitor the efficiency of the polarizer during data taking. Similar measurements of the liquid hydrogen target transmission, made using the intermediate and back beam monitors, will be used to monitor the target (ortho-para) hydrogen ratio. The back monitor will also play an important role in the calibration of the RF spin flipper efficiency, using the ^{3}He polarization analyzer.

3.1.9 WBS 1.9 — Cave

The cave work package consists of different shielding structures in ER1 — the guide tunnel, the experimental cave, and the beam stop, as shown in Fig. 9. The shielding is needed to protect personnel from radiation. The shielding of the experimental cave also has to shield the experiment from ambient AC and DC electromagnetic backgrounds. DC magnetic fluctuations in the experimental cave location have been measured to be at the level of 10–20 mG. The facility requirement for the dose levels outside the radiological shielding in ER2 is 1 mrem/hr. The magnetic shielding of the cave is integrated with the cave radiological shielding.

The radiological shielding has been designed by experts at the LANSCE facility, using computer codes that have been tested on other flight paths. An official approval process of the FP12 radiological shielding is in process. One of the safety factors in the shielding design is that the shielding calculations have been done for 200 μA average proton current, though the facility is unlikely to run with more

than 150 μA proton current.

Guide tunnel

The 8 m long guide tunnel starts from the ER1/ER2 wall. Two types of shielding approaches have been used, with a goal of optimizing cost. Next to the ER1/ER2 wall is a 3 m length of heavier shielding. Because of a lack of floor space, steel-poly combination shielding will be used, which will keep the thickness of the shielding walls small (12"). This section of the shielding is under construction. To gain more floor space in ER2, FP12 and FP13 will have a common wall from the ER1/ER2 wall to the FP12 cave.

The last 5 m length of the guide tunnel will be constructed using 15–18" thick magnetite concrete blocks with a single layer of borated poly on both sides. The procurement process of the concrete blocks is ongoing.

Experimental cave

The neutron guide ends at 21 m from the source and the center of the experimental cave is 22 m from the source. The cave will house the NPDGamma apparatus, electronics, and also two clean power transformers. The cave has to allow installation and removal of the apparatus. The roof of the cave will serve as a working platform where many of the components of the experiments will be located, for example the gas handling system of the liquid hydrogen target. The cave has to shield the experiment against ambient EM noise of ER2 and it has to protect personnel outside the cave against radiation.

The original design of the cave shielding used metal cans filled with 8" of poly. The cans were made from 1/4" thick steel. With these elements the cave wall and the roof construction would be simple. This approach has been used in the other flight paths of the facility. This shielding design would meet the radiological and our preliminary EM shielding requirements, based on shielding the earth's magnetic field.

However, this shielding would be inadequate to attenuate the fringing field of the recently commissioned FP11A 11 T superconducting magnet. Some local shielding has been placed around the FP11A magnet to reduce its stray field. Without any FP12 shielding, we have measured the field to be 800 mG at the location of the middle of the cave when the FP11A superconducting magnet was fully charged. To protect the experiment from this field, we need a shielding factor of over 100. We have investigated several shielding solutions, with the conclusion that it is not possible to construct magnetic shielding around the experiment that has a shielding factor of over 100 while remaining within our budget. We cannot simply increase the thickness of the steel because a 200 ton shield that provides only a shielding factor of 15 is already at 75% of the ER2 floor loading limit.

We have pursued magnetic shielding design using both three-dimensional numerical modeling and an analytical approach. We have built a small-scale cave mock-up to verify shielding predictions, and we have also measured μ-values for different steels in order to evaluate possible shielding efficiencies.

Since it is not possible to find a rational technical solution for shielding the NPDGamma experiment against the existing fringing field of FP11A, we have worked with LANSCE Division to find a solution that allows both experiments to pursue their physics objectives without sacrificing any goals. Various engineering and administrative solutions and combinations have been considered.

We are ready to begin detailed engineering design as soon as we have a solution for handling the fringing field of FP11A. We have lost several months with this problem. If we do not have a solution soon, we will have serious difficulties in meeting our schedule of commissioning the experiment and starting data taking.

Beam stop

The beam stop has been designed and procurement has been started. The beam stop has been approved by the LANSCE Radiation Safety Committee.

3.1.10 WBS 1.10 — ER2 Utilities

Utilities for ER2 consist primarily of electrical power. Since this is a new beam line, no such utilities exist and power at 480 V must be brought from the main electrical room, converted to the appropriate voltages, and distributed to the branch circuits.

Four transformers are used to convert the incoming 480 V power to 208 and 120 V power for the experiment. Two transformers provide power to equipment located outside the cave, providing separate clean (15 kVA) and dirty (30 kVA) power. Two 15 kVA transformers provide a similar system for powering equipment inside the cave. All four transformers feed breaker panels that supply the branch circuits. All design work is performed by qualified facility engineers and all installation work by qualified electricians.

At present a 480 V panel and 400 A breaker to provide power to the experiment and beam line have been installed. A conceptual design of the remaining work is also complete. The main risk associated with this work is due to the tight schedule coupling with the construction of the cave. We are working closely with LANSCE engineers to mitigate this risk.

3.2 Status of the NPDGamma Beam Line Construction Project

The NPDGamma collaboration is also responsible for building the new cold neutron beam line for fundamental nuclear physics. FP12 at the Manuel Lujan Neutron Scattering Center was allocated for this purpose. The agreement is covered by a MOU between the LANSCE and Physics Division. The allocated FP12 consisted of only a core drilled hole filled with shielding material in the biological shield viewing the new upper tier cold hydrogen moderator of the spallation source. The NPDGamma collaboration has to build the neutron guide from the moderator to the experiment, the external shutter (outside the biological shielding), the frame definition chopper, and the radiological shielding around the beam line in ER1.

Simultaneously with the FP12 construction, the adjoining FP13 is under construction by LANSCE Division. The construction of these two beam lines has been a collaborative effort between Physics and LANSCE Divisions and coordinated by LANSCE. This integrated construction approach was one of the recommendations of the Spinka I Committee. The goal of the collaborative effort has been to save resources, since many of the beam line components are similar and also the front end shielding of these beam lines had to be integrated because of the lack of the space between them. The collaborative effort also has its difficulties, one of the basic problems being that the funding sources of the beam lines projects are different, leading to scheduling problems. LANSCE and Physics Divisions have cooperated to solve these problems.

The schedule of the beam line construction depends upon the facility schedule — most work can be done only when the beam is off for facility maintenance breaks.

3.2.1 WBS 2.1 — In-Pile Guide

The in-pile part of the neutron guide system comprises the 4 m long guide, the steel insert that supports the guide and allows guide alignment, and the thimble — a vacuum jacket that isolates the spallation source vacuum from the guide vacuum.

For statistics the experiment requires all available neutrons, i.e. as large a neutron guide inner

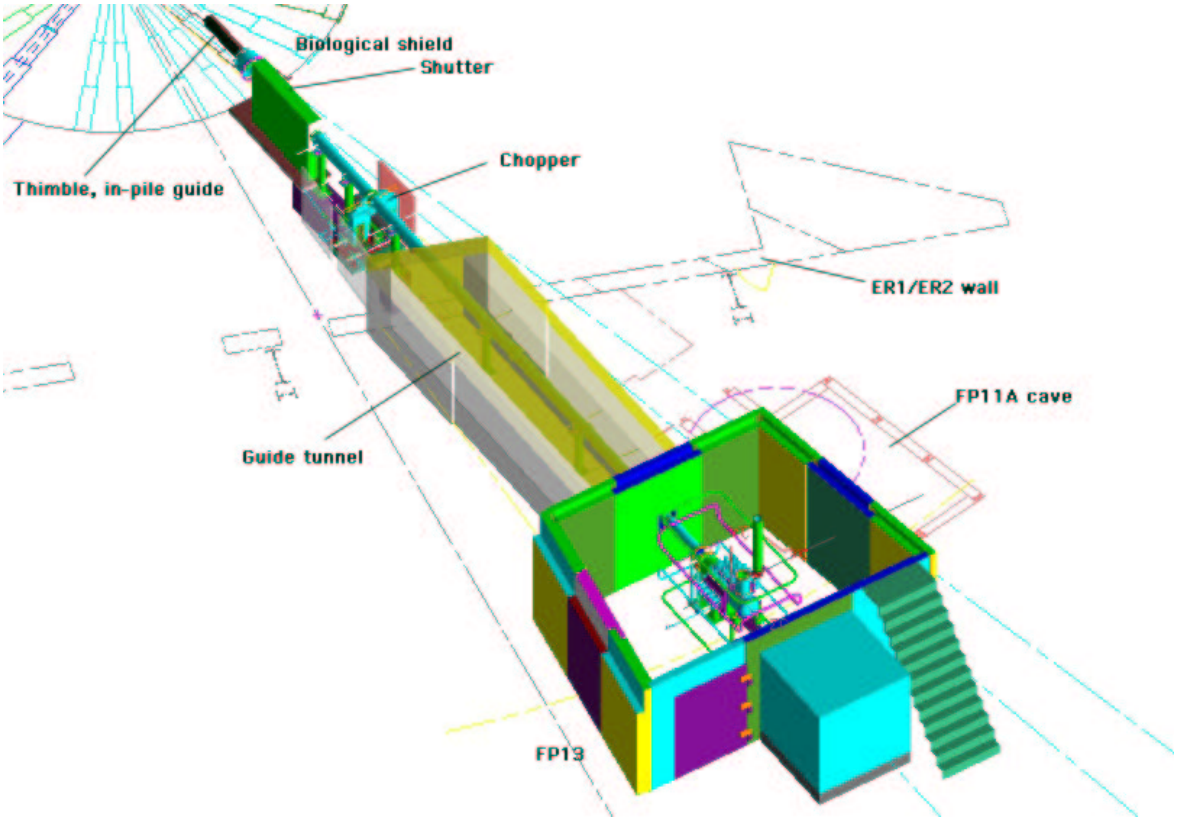

Figure 9: Isometric picture of the beam line and the NPDGamma experiment. Integrated shielding in ER1 is not shown.

cross section as possible. The largest guide that could fit into the hole in the biological shield has a cross section of 9.5×9.5 cm^2. This size of guide was only possible if the section of the guide next to the source was cantilevered (about 2 m out of 4 m). The mechanical strength of the thimble had to meet nuclear facility CAT III requirements. The thimble had to be built to fit precisely the existing FP12 liner inside the bulk shield.

The supermirror coatings of the in-pile guide are specified to have a reflectivity of $\Theta_c = 3\times^{\text{nat.}}\text{Ni}$. The coating and the glass substrate have to survive in the radiation field of the spallation source. In addition, the energy deposit of the radiation should not elevate the temperature of the guide to the level where the coated layers could diffuse and thus cause a loss of reflectivity. During the previous LANSCE run cycle a thermocouple system was installed into the thimble and temperatures monitored during different operating modes of the source. No significant increase in temperature was noticed. The in-pile guide has to hold its precision alignment for several years.

The reflectivity of the coatings was tested by the manufacturer, MIRROTRON Ltd., in a neutron beam in the Budapest Research Reactor. According to the data sheets the coated guide sections meet specifications. Careful alignment of the guide was performed during the installation.

A part of the beam line commissioning is a measurement of the guide performance. The measurement has been scheduled for late 2002 or for the time when the beam comes back after the 2003 facility maintenance break in July. During our test runs on FP11A we measured the moderator brightness and studied the guide performance. The same technique can be used for FP12. To keep the temperature of the guide under control, the in-pile guide, shutter guide, and the guide section between the shutter and chopper will be filled with ^{4}He gas. The risks of the in-pile guide are: a long-term loss of reflectivity because dose rates are faster than estimated, and a loss of alignment caused by a change in the mechanical support structure.

3.2.2 WBS 2.2 — Shutter

The biological shield of FP12 has no room for a shutter. Therefore, the first external shutter in the MLNSC facility was designed and constructed. The function of the shutter is to stop the beam when in the closed position so that personnel can work in the experimental cave. In the open position, the shutter neutron guide has to align to the rest of the neutron guide. The shutter block, moved by a hydraulic system, is about 2 m long and weighs about 2.5 tons. The neutron guide is filled with ^{4}He gas. The shutter and the neutron guide in ER1 have to be isolated from the unstable ER1 floor. This was accomplished by cutting the floor and installing concrete pillars that are isolated from the floor on the base plate under ER1. The shutter is part of the facility safety system.

The shutter operation has to be reliable and the shutter guide has to meet alignment requirements after years of operation. Numerous shutter operations were performed on the bench and after the installation on the beam line. These tests confirmed the reliability and repeatability of the shutter.

The shutter was installed during Spring 2002. The shutter will be further tested and commissioned either at the end of 2002 or immediately when beam comes back after the 2003 facility maintenance break in May 2003. The major risks are that the shutter guide can slowly lose its alignment or there will be a leak in the hydraulic system that prevents the operation of the shutter. To fix these problems the integrated shielding has to be opened to access the shutter. This would be a major operation that will also affect adjoining beam lines. Therefore, the design of the shutter emphasized reliability.

3.2.3 WBS 2.3 — Chopper

The analysis of NPDGamma data requires accurate knowledge of the neutron beam energy incident on the LH_2 target as a function of time. The distance of the target from the moderator, 22 m, is great enough that neutrons from previous neutron beam pulses can overlap with succeeding pulses before they reach the target, thereby destroying time of flight information. In order to eliminate this frame

overlap, a beam chopper must be installed upstream in the beam line at a point where the neutron beam pulses are still spatially resolved. The frame overlap chopper will filter out neutrons with energy less than $E_{\rm n} < 1.5$ meV. Time of flight for these neutrons at 22 m is longer than the beam pulse period (50 ms). The second task of the frame overlap chopper is to define the time-of-flight range in a neutron pulse where the gamma-ray asymmetry will be measured. For captured neutrons with energy greater than 15 meV, depolarization will occur in liquid para-hydrogen by spin-flip scattering and therefore no parity violation can occur.Neutrons with energies less than 15 meV do not have enough energy to depolarize by flipping the proton spin and will therefore show a PV effect.This has led us to the following DAQ strategy per neutron pulse; from 0–10 ms after a proton pulse when the neutron energy is higher than 15 meV, the collected data is used to measure a null result. Then from 10–28 ms the chopper is open and the collected data is used to determine the PV gamma-ray asymmetry, and finally at 28 ms the frame definition chopper will shut off the beam and data are collected from 28 ms to the end of the 20 Hz frame to determine the beam-off background

The frame overlap chopper consists of a rotating 1 m diameter disk powered by an electric motor. Neutrons are absorbed by a thin layer of ^{203}Gd applied to the surface of the rotor. The rotor has an aperture that allows the neutrons of interest to pass through. The phase of the rotor relative to the beam pulse is maintained by an electronic feedback control. Two entirely independent frame overlap chopper systems will be installed in ER1 part of FP12 to provide redundancy in the event of a failure.

The FP12 frame overlap chopper system is completely machined and has been delivered to Los Alamos. The rotors were successfully coated during Summer 2002. The control system has been demonstrated. Further minor incremental improvements in the mechanical and control systems will be made prior to the planned installation in February 2003.

There are three performance requirements for the chopper. The first is that the chopper has to absorb the unwanted slow neutrons from beam. The second is that the control system must maintain a phase accuracy that is small compared to the data acquisition sampling interval. The third requirement is that the chopper be reliable to operate. To address the first requirement, we requested and received beam time for Fall 2002 from the LANSCE PAC at the MLNSC to test samples of the coated rotor material. The testing is completed and the results indicate that the coatings meet specifications. The vendor who coated the rotors claims prior success for similar applications.

The data for the experiment will be recorded with a time resolution of at most 100 μs. We therefore define the phase-locking requirement for the chopper to be on the order of 10 μs. This performance requirement is fairly relaxed compared to that of other chopper systems already in service at the Lujan center that have achieved phase-locking sigmas of less than 1 μs (for rotors with a much higher moment of inertia).

A TTL veto signal will be updated every beam pulse to signal whether the rotor phase is within programmed limits. In addition, detailed pulse-by-pulse performance data will be broadcast to the DAQ over Ethernet using the TCP protocol. These data can be saved in files on a run-by-run basis for later analysis.

The chopper system is currently assembled and tested at LANSCE. It has been operated at 20 Hz to test the rotor balance and the control systems. The chopper design is consistent with many other chopper systems that run successfully at MLNSC. In the chopper design, reliability has been one of the main issues. We anticipate no problems installing, commissioning, or running the chopper system.

3.2.4 WBS 2.4 — Integrated Shielding

Neutron pulses from a spallation source also include fast neutrons in the keV–MeV range. Stopping of these neutrons requires thick shielding. Typical radiological shielding at a spallation source is comprised of layers of steel and regular and borated polyethylene. The necessary thickness of shielding layers is defined by the dose limits given by the facility. The dose rate outside the shield has to be less than 2 mrem/hr in ER1.

Because of the close proximity of FP11, FP12, and FP13 in ER1, it was necessary and cost effective to cover these beam lines with integrated shielding, instead of building individual shielding packages around the beam lines. The design of the shielding is based on numerical modeling. The models have been used for the shielding calculations of the other flight paths in the facility. In Spring 2002 the integrated shielding was completed, allowing beam to be turned on.

In February 2003 a part of the shielding must be removed in order to install the chopper and the last ER1 guide section.

3.2.5 WBS 2.5 — Neutron Guide

The total length of the FP12 neutron guide is 20 m. The first 8 m has been installed, including the in-pile guide, the shutter guide, and the 2 m section from the shutter to the chopper. These three sections of the guide are coupled to form a single volume that will be filled with ^{4}He. The last 12 m of the guide will be operated in vacuum.

The guide has an inner cross section of 9.5×9.5 cm^2. This supermirror guide is assembled of 50 cm long glass sections. The glass pieces are coated by over 600 Ni and Ti layers, giving a reflectivity of 3 times that of natural Ni. The glass pieces are mounted into a heavy vacuum tube. Fig. 10 shows the assembled 12 m long guide vacuum tube in the factory at MIRROTRON Ltd. in September 2002. A 1.2 m long part of the neutron guide extends into the experimental cave. Because of the homogeneity requirements of the guide field, the vacuum tube of the guide has to be made from stainless steel.

In September most of the glass pieces were cut and some of them were already coated. The next step will be to test the reflectivity of the coatings in the Budapest Research Reactor and then start the assembly of 50 cm long guide units. The shipping of the guide system will take place in December and the installation and precision alignment can start as soon as the beam is off, the integrated shielding opened, and the chopper installed which will take place in February 2003.

This schedule can tolerate possible delays. The installation of the guide has to be completed and the integrated shielding reinstalled before the facility can turn the beam on. The 1L target tuning will start in May 2003. The installation of the guide and the cave construction are not strongly coupled.

Figure 11 shows calculated neutron flux at the end of the guide as a function of time of flight when the average proton current is 150 μA.

3.2.6 WBS 2.6 — ER1 Utilities

Modifications had to be made in ER1 to existing utilities. Some of the power and facility control signal lines had to be removed to more convenient locations. Our ER1 beam line components will be powered from our ER2 utilities, especially 480 V and 208 V three-phase power.

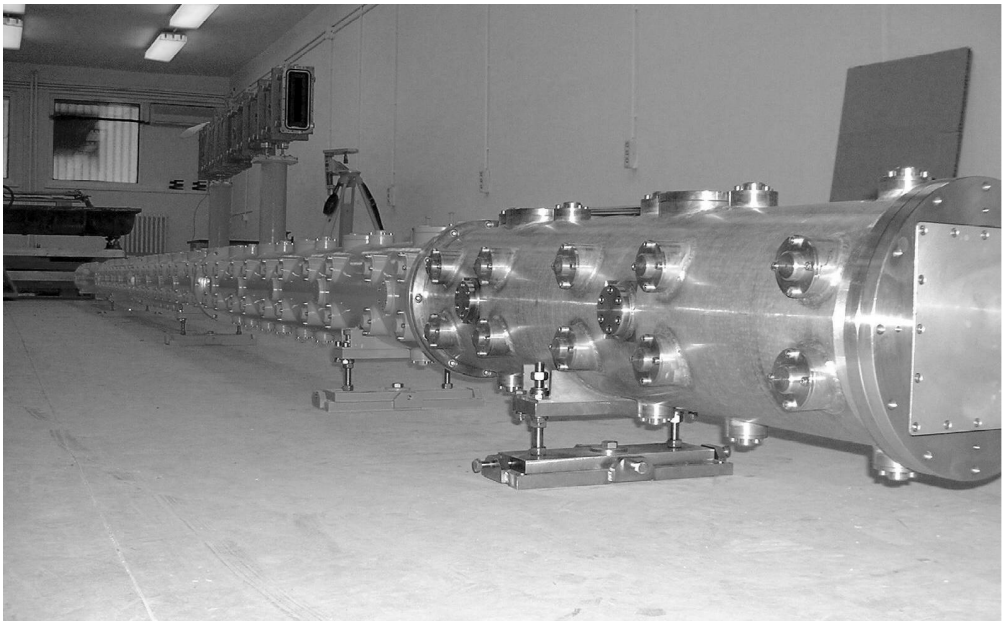

Figure 10: The assembled 12 m long neutron guide vacuum tube in the factory. The last 1.2 m has been made from stainless steel. The numerous access ports are for alignment, both view ports and alignment screws.

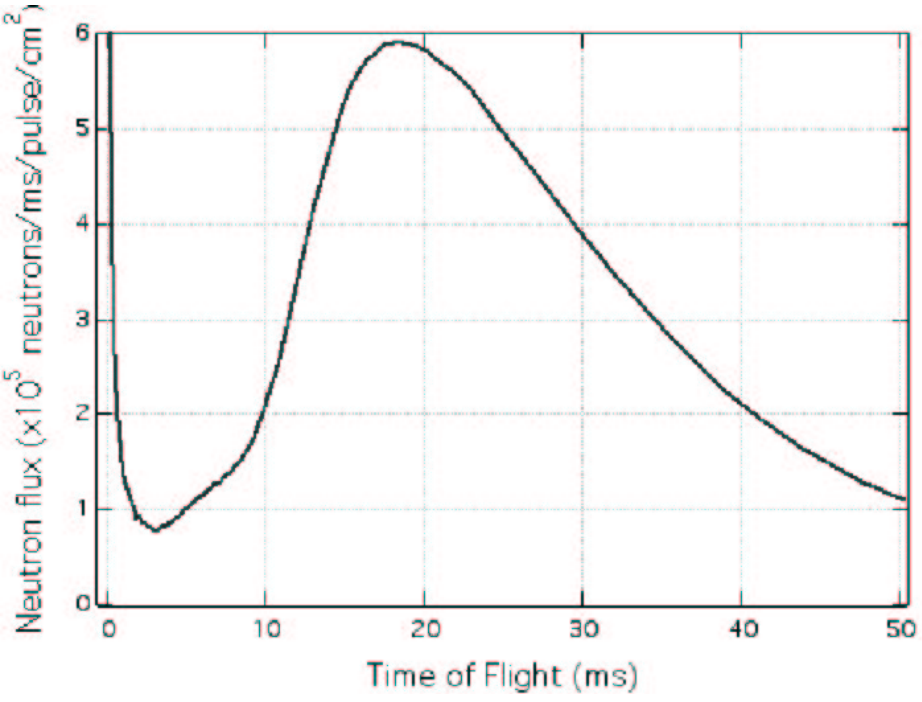

Figure 11: Calculated flux of FP12.

4 Updates to Statistical and Systematic Errors

Statistical and systematic errors are throughly discussed in Section 4 of the NPDGamma proposal. Most of this discussion remains valid. Many open issues, some of them raised by the reviews, were resolved in test runs carried out in Fall 2000 and Fall 2001. Some of the results of the test runs are discussed in a draft of an article to be submitted for publication. The draft is Appendix F of this report.

4.1 Statistical Errors

In the Fall 2000 test run we measured the brightness of the FP11A moderator. The measured brightness agreed with Monte Carlo simulation of the brightness performed by the facility to within 10%. There is good reason to believe that the moderator brightness for FP12 predicted by the same Monte Carlo simulation will realistically predict our beam intensity on FP12, which views a different moderator than FP11A.

The NPDGamma experiment has been designed to measure A_γ with a precision of 1.5×10^{-8} in 2×10^7 seconds at 200 μA proton current on the MLNSC 1L target. With a proton beam current of 120 μA and 2500 hours/year, 3.7 calendar years will be required to collect statistics.

The Fall 2000 test run addressed the issue of neutron beam position fluctuations produced by density fluctuations in the moderator. Beam position changes can affect the observed asymmetry. Since the moderator fluctuations are not spin correlated, the effect averages to zero. The fluctuations do, however, add noise to the asymmetry measurement. The moderator is not expected to bubble because it is operated in a supercooled gaseous state. However, we wanted to establish experimentally that up-down position motion of the neutron beam at the experimental target will introduce negligible noise into the asymmetry measurement. Because the supermirror guide strongly washes out position fluctuations, moderator density variations are primarily observed as intensity fluctuations. Since the relationship between intensity and position fluctuations is a function of the guide geometry, a measurement of of position fluctuations can be used to determine the size of position fluctuations. During the Fall 2000 test run we measured fluctuations in the ratio of neutrons/proton current. The inferred upper limit on up-down position fluctuations was 10 times smaller than required.

We have measured the number of photoelectrons/MeV from the CsI coupled to VPDs and the preamplifier noise. The the preamplifier noise is 20 fA/$\sqrt{\text{Hz}}$ as expected and the photocathode current is ~ 3 times larger than in the proposal because the CsI crystals purchased are heavily Tl doped for radiation damage resistance. We expect to meet or exceed the time estimates in the proposal for demonstrating that additive and multiplicative false asymmetries are negligible. We will be able to quickly measure these false instrumental asymmetries and troubleshoot them.

The Fall 2000 test run included data taking with what was essentially a 10% scale model of the full NPDGamma experiment. During the test run we studied PV asymmetries on Cd, Cl and La targets with an uncertainty level of 2×10^{-6}. These measurements demonstrated the ability of the system to operate at neutron statistics.

4.2 Systematic Errors

In the proposal we identified two types of systematic errors:

- systematic errors of instrumental origin and
- systematic errors from couplings to the neutron spin other than the $\sigma_n \cdot \vec{k}_\gamma$ correlation we seek to measure.

4.2.1 Type 1 — Systematic errors of instrumental origin

We have worked hard to reduce false couplings. We will have an isolated ground for the experimental cave that forms a Faraday cage around the apparatus. The fast sampling ADCs that receive the preamplifier signals are in their own VME crate that is coupled to the DAQ by fiber optic. The RF spin flipper currents are well shielded by a twin-lead coax cable. VPDs were chosen for their immunity to magnetic fields. Turning the RF spin flipper on and off effects the PV signal in second order through magnetic coupling between the spin flipper and the VPDs. We have measured the second order VPD gain shift to be $1 \times 10^{-5}/\mathrm{G}^2$. Thus if the stray field from the RF spin flipper at the VPDs is less than 5 mG, the effect on the asymmetry will be negligible. We will measure the spin flipper leakage field and demonstrate it to be negligible. Any effect will be observable using LED signals and by taking data with no signal, measuring the asymmetry in the electronic noise.

4.2.2 Type 2 — Systematic errors from couplings to the neutron spin

These asymmetries are enumerated in Section 4.2.2 of the proposal and the discussion remains valid with two benign exceptions. As discussed in the target section of this report (Section 3.1.7), we have switched from a Mg to a Ti target vessel. Titanium, like magnesium, has a negligible level of false asymmetry from capture gammas from polarized neutrons.

In the Fall 2000 test run we discovered that the feedthrough pins of the VPDs were ferromagnetic. We made a careful calculation of the effect of the analyzing power of the polarized electrons in the pins for the parity-allowed circular polarization of the 2.2 MeV gammas. The effect was negligible for the following reasons: the transfer of neutron polarization to gamma circular polarization is small ($\sim 1.3 \times 10^{-3}$), the mass of the pins is small (~ 1 g/VPD), the pins are shielded from the 2.2 MeV gammas by the CsI, the analyzing power for back scattered gammas is about 30 times smaller than for forward scattered gammas, and finally the energy of the back-scattered gammas is small (~ 250 keV). We also carefully calculated the false asymmetry from iron in the cave and showed that it is small.

4.2.3 Spin Reversal

As discussed in the proposal, we use an 8-step sequence for reversing the neutron spin with the spin flipper for each pulse, which cancels drifts in the measured asymmetry to quadratic order in time.

We have three methods of spin reversal: RF spin flipper, adiabatic fast passage reversal of the ^{3}He polarization, and reversal of the guide field direction. The experiment will reverse the spin on a pulse-to-pulse basis using the RF spin flipper. We will periodically reverse the ^{3}He polarization depending on the loss of polarization (estimated to be $\sim 1\%$/reversal). The least frequent reversal will be done using the guide field. In addition, we will study the observed asymmetry as a function of time of flight as discussed in the proposal. These tests provide a tight sieve for various sources of Type 2 false asymmetries. We do not intend to make cuts on the data other than for unstable operating conditions. We expect the pulse to pulse and run to run fluctuations to be Gaussian and to be dominated by counting statistics provided that the operating conditions are stable. We will check this assumption in the distribution of observed asymmetries.

4.2.4 Stability of operating conditions

In addition to statistical and systematic errors, we are concerned about stable operating conditions. We plan to monitor ambient conditions such as neutron beam current, temperatures, line voltage, neutron energy spectrum, and ambient magnetic fields, and to correlate them with possible anomalies in the data. The stray magnetic field from the FP11A superconducting magnet is of particular concern. The efficiency of the (resonant) RF spin flipper is strongly dependent on any changes in the 10 G guide field. An 18 mG change in the guide field changes the RF spin flipper efficiency by 10%, the

goal statistical error. As this report is being written we are working with the LANSCE Division to insure that the influence of the stray field from the FP11A magnet will not exceed 6 mG (2% change in the efficiency).

5 Status of Costs and Schedules of the Projects

The NPDGamma Project consists of two projects:

- Experiment Construction Project
- Beam Line Construction Project

These projects are managed according to the "$\vec{n}+p \rightarrow d+\gamma$ Project Management Plan for Experiment and Beam Line Construction" (PMP) (Appendix B). The PMP describes the management structure, sets the rules and gives the work breakdown structure (WBS) that is the basis for the cost structure and schedule organization. Basic management elements are 16 Work Packages lead by work package leaders.

The PMP describes the cost and schedule baselines, major milestones, and budget profiles. The PMP explains controls used to manage the projects:

- Management control
- Technical control
- Cost and schedule control
- Performance control
- Contingency management
- Progress reporting

Reporting has been the main element in following the progress of the projects. The work package leaders send status reports to the Project Manager who then reports to the LANL management and compiles the quarterly reports to DOE.

5.1 Status of Experiment Construction

5.1.1 Status of the Budget for the Experiment Construction

The experiment construction project is funded by several sources. The funds come from DOE, LANL, NSF, NSERC (Canada), KEK (Japan), and from universities. Most of the components of the experiments have been procured, are under construction, or have already been delivered to LANL.

Table 3 shows a summary of the DOE funds for experiment construction. Figure 12 show the actual expenditure rate compared to a linear prediction for the DOE funds. Table 4 gives base costs, expenditures, and status of contingencies per work package.

	$k	
Total Baseline	1,316	
YTD DOE allocations	1,218	
Costs and commitments (FY98-FY02 4th quarter)	536	
Remaining contingency	181	17%

Table 3: Summary of experiment construction expenditures.

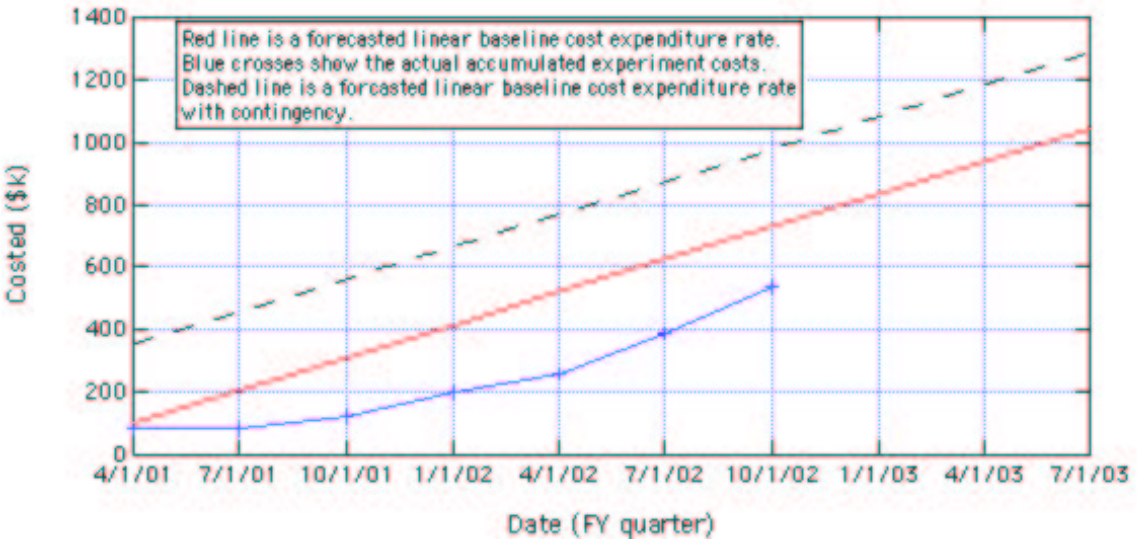

Figure 12: The forecasted linear spending rate of the baseline cost and the actual costs for experiment construction.

WBS	Element	Costed & Committed	Estimate to Complete	Total Base Cost	Available Contingency	% of Total Base Cost
1.1	Signal Electronics	9	31	40	11	28%
1.2	Data Processing	19	53	72	6	8
1.3	Detector	130	31	161	13	8
1.4	^{3}He Polarizer	5	12	17	2	12
1.5	Spin Flipper	17	6	18	2	11
1.7	LH2 Target	88	19	88	12	14
1.9	Cave	227	383	544	115	21
1.10	ER2 Utilities	41	52	93	14	15
1.11	Commissioning	0	11	11	6	55
	Totals	536	598	1044	181	17%

Table 4: Budget status (in $k) of the experiment construction work packages for the DOE funds. The first column indicates costed and committed funds. The second column shows the cost estimate to complete the project and the third column gives the baseline. The fourth and fifth columns give the remaining contingencies and percentage of the contingencies from the base cost.

5.1.2 Major Changes to the Experiment Construction Baseline

The following major changes have been made to the baseline design that have affected the schedule or costs.

WBS 1.3 — Detector The set of CsI crystals weighs about 0.7 metric tons. The detector has to be capable of moving in the $x-y$ plane to align the detector with the guide field. This required a more complicated stand than we had in the baseline. Our Canadian collaborators have taken responsibility for funding and constructing the new stand.

WBS 1.9 — Cave A change to the baseline design unknown at this moment. We are still looking for a solution to the FP11A fringing magnetic field issue. From the baseline the cave was moved an additional 3 m back to increase the distance to the FP11A magnet. This caused cost increases in the estimates of the guide tunnel and cave construction, but so far the costs are still within work package contingencies.

WBS 1.10 — ER2 Utilities This is the electrical power for the experiment (see Section 3.1.10). The power required was not available in ER2 and the project had to install a power feed to the experiment. The increase in cost was within the work package contingency.

5.1.3 New Major Milestones to Complete the Project

To complete the project, the components have to be completed, tested, shipped to LANL, assembled and tested at LANL, and then installed in the cave and commissioned. The new schedule has been created and the major milestones have been listed below. The goal of this schedule is to allow the experiment to be in production during October–December 2003 before the beam will be off for the 2004 maintenance. The cave introduces an uncertainty to this schedule.

Major new milestones:

WBS 1.1 — Signal electronics

1. Preamplifiers built 11/30/02
2. SD amplifier built 2/28/03
3. VPDs, CsI crystals and preamps matched 12/30/02
4. Testing of detector electronics on bench completed 3/28/03

WBS 1.2 — Data processing

1. VME station 3 ready 12/30/02
2. Complete DAQ system ready and tested 2/28/03
3. Decision of data storage format 4/15/03
4. Completed testing of DAQ in ER2 with detector in the cave 5/30/03

WBS 1.3 — Detector

1. Assembly of VPDs, preamp, and crystals completed 12/29/02
2. Stand completed at TRIUMF 12/29/02
3. Arrival of the stand at LANL 1/15/03
4. Stand assembled and tested at LANL 2/12/03
5. Installation of stand in cave 4/29/03
6. Detector commissioned with beam 8/30/03

WBS 1.4 — Polarizer

1. Polarizer
   (a) Test of polarizer at U. Michigan completed 12/13/02
   (b) Polarizer shipped to LANL 1/24/03
   (c) Polarizer testing at LANL completed 3/15/03
   (d) Polarizer installed and tested in the cave 5/30/03
   (e) Polarizer commissioned with beam 8/15/03
2. Analyzer
   (a) Analyzer designed 12/24/02
   (b) Analyzer tested at UNH 2/25/03
   (c) Analyzer at LANL 3/15/03
   (d) Analyzer tested at LANL in laser lab 5/15/03
   (e) Analyzer tested in the cave with beam 8/29/03

WBS 1.5 — Spin Flipper

1. SF built 11/30/02
2. SF tested with the DAQ and detector in lab 1/29/03
3. SF spin flip efficiency test complete 8/18/03

WBS 1.6 — Guide Field

1. Guide field coils assembled and tested at UC-Berkeley 1/29/03
2. Guide field components at LANL 2/15/03
3. Assembly at LANL and testing completed 3/15/03
4. Installation in cave and testing and field mapping completed 4/28/03

WBS 1.7 — Target

1. Target built 2/15/03
2. Gas handling system built 2/15/03
3. Testing at IUCF completed 3/15/03
4. Target at LANL 4/1/03
5. H_2 supply system built 4/1/03
6. Exhaust line in ER2 constructed 4/15/03
7. Target installed in the cave 5/1/03
8. Passed target operational safety review 5/1/03
9. Passed target readiness review 5/15/03
10. Target fully tested in cave without beam 6/1/03
11. Target tested with beam 8/29/03

WBS 1.8 — Beam Monitor

1. Testing in FP5 completed 12/16/02
2. Preamplifiers built and tested 2/15/03
3. Installed in the cave 5/15/03
4. Tested in the cave with beam 7/29/03

WBS 1.9 — Cave

1. Guide tunnel
   (a) Laminated section installed 3/15/03
   (b) Concrete blocks arrived and installed 3/31/03
   (c) Guide tunnel completed 4/15/03
2. Cave
   (a) Agreement on concept for cave shielding 11/29/02
   (b) Detailed shielding design completed 1/20/03
   (c) Procurement completed 2/28/03
   (d) Installation completed 4/30/03

WBS 1.10 — ER2 Utilities

1. Detailed design completed 1/30/03
2. In ER2 480V panel and transformers installed 3/15/03
3. Load wiring done 4/28/03

5.2 Status of Beam Line Construction

5.2.1 Status of the Budget for Beam Line Construction

The beam line construction project consists of the FP12 beam line components and shielding in ER1. The beam line construction is fully funded by DOE except for the chopper, which is partly covered by University of New Hampshire collaborators. Most of the beam line is costed or committed. The main effort left is to open the integrated shielding in ER1 and install the chopper and the neutron guide and then close the shielding. Table 5 shows a summary of the beam line construction budget. Figure 13 shows the actual expenditure rate compared to a linear prediction. Table 6 gives base costs, expenditures, and status of contingencies per work package.

	$k	
Total Baseline	1,908	
YTD DOE allocations	1,908	
Costs and commitments (FY98-FY02 4th quarter)	1,716	
Remaining contingency	83	5 %

Table 5: Summary of beam line construction expenditures.

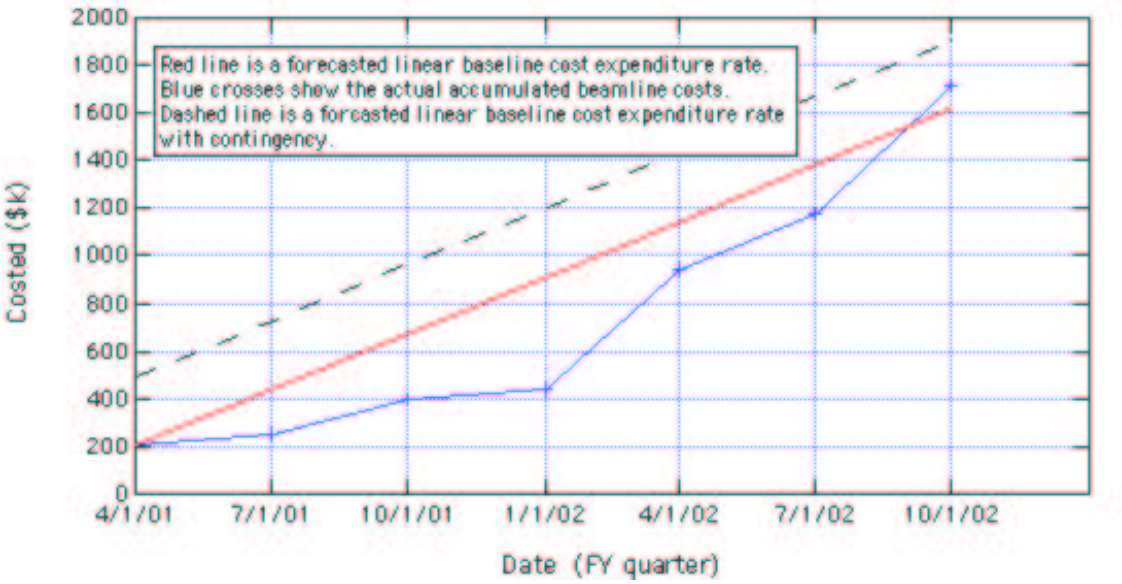

Figure 13: Actual spending rate and the forecasted linear rate.

WBS	Element	Costed & Committed	Estimate to Complete	Total Base Cost	Available Contingency	% of Total Base Cost
2.1	In-Pile	101	0	82	2	2%
2.2	Shutter	203	0	159	0	0
2.3	Chopper	98	0	87	0	0
2.4	Integrated Shielding	595	9	477	6	1
2.5	Neutron Guide	698	54	750	49	7
2.6	ER1 Utilities	21	31	49	19	39
2.7	Commissioning	0	14	14	7	50
	Totals	1716	108	1618	83	5%

Table 6: Budget status (in $k) of the beam line construction work packages for the DOE funds. The first column indicates costed and committed funds. The second column shows the cost estimate to complete the project and the third column gives the baseline. The fourth and fifth columns give the remaining contingencies and percentage of the contingencies from the base cost.

5.2.2 Major Changes to the Beam Line Construction Baseline

The only change to the baseline design was to increase the length of the neutron guide by 3 m. With this increase we obtain more distance from the FP11A magnet and obtained also the possibility of constructing a larger experimental cave.

WBS 2.5 — Neutron Guide The extra 3 m section of guide was purchased to increase the distance from the FP11A magnet. The costs stayed within the contingency.

5.2.3 New Major Milestones to Complete the Beam Line Construction

A new schedule has been created for the beam line construction. Below are the proposed milestones. The assumption is that the beam delivery to the 1L target will stop at the end of January 2003. This will allow us to start opening the integrated shielding in ER1 for chopper and guide installation.

Major milestones:

WBS 2.1 — In-pile guide

1. Commissioning completed 7/29/03

WBS 2.2 — Shutter

1. Gas handling system complete 5/18/03
2. Commissioning completed 7/30/03

WBS 2.3 — Chopper

1. Chopper bench testing at LANL completed 12/31/02
2. Chopper installed to beam line 3/4/03
3. Chopper testing in beam line completed 3/21/03
4. Commissioning completed 7/30/03

WBS 2.4 Integrated shielding

1. Start to open the integrated shielding 2/1/03
2. Integrated shielding closed 5/19/03

WBS 2.5 — Neutron guide

1. Reflectivity measurements of coatings completed 12/29/02
2. 50 cm long sections assembled 12/29/02
3. Guide system at Los Alamos 1/15/03
4. Installation completed 3/15/03
5. Commissioning completed 8/4/03

WBS 2.6 — ER1 utilities (Completed.)

APPENDICES

A NPDGamma Proposal

(see attached)

B Management Plan

(see attached)

C Schedules

(see attached)

D Draft Commissioning and Operations Plan

(see attached)

E Draft Agreement Between Physics and LANSCE Divisions

(see attached)

F Draft Article of Fall 2000 Test Run Results

(see attached)

G Publication List

(see attached)